

Fifth Force

R. L. Mills, Y. Lu

BlackLight Power, Inc., 493 Old Trenton Road, Cranbury, NJ 08512

ABSTRACT

Mills [1-11] solved the structure of the bound electron using classical laws and subsequently developed a unification theory based on those laws called Classical Quantum Mechanics (CQM) with results that match observation for the basic phenomena of physics and chemistry from the scale of the quarks to cosmos. That space provides an absolute velocity c based on its intrinsic permittivity ϵ_0 and permeability μ_0 is generalized from Maxwell's light-front equation to all fields traveling with limiting velocity including the gravitational field which predicts that with particle production a physical alteration in nature of space occurs that is described by a modified Schwarzschild-type metric, and leads to a physical basis of gravitation, the identity of absolute space, and the nature of absolute versus relative time dilation for accelerated matter that is returned to be coincident with twin matter. Some of the results are the predictions of the masses of all of the fundamental particles, the fundamental cosmological parameters, and the acceleration of the expansion of the universe that match observations. The basis of inertial mass including its equivalence with the gravitational mass is given in terms of the particle production condition for bound matter. Uniquely, a further prediction is a zero gravitational mass of the photon and the free electron that is confirmed by experimental data in the literature. A further prediction is that a special free state of the electron called a hyperbolic electron can be formed having a captured photon, and the force between a gravitating body and such an electron state is in the opposite direction with orders of magnitude greater acceleration than that of the gravitational force on ordinary bound states of matter. This paper is the second in a series of two that covers two specific predictions of CQM: (1) the existence of lower-energy states of the hydrogen atom which may be the dark matter and is the product of a new chemical energy source reported in the first, and (2) the existence of a fifth force beyond the electromagnetic, strong and weak-nuclear, and gravitational forces reported herein. Specifically, we report the experimental confirmation of 15 predicted hyperbolic-electron states that are observed forced away from the Earth with an acceleration that is over twelve orders of magnitude greater than that of gravity as predicted.

Keywords: special and general relativity, twin paradox, absolute space, gravitation, cosmology, electrons, fifth force

I. Introduction

A. Absolute Space and Relativity

Maxwell's electrodynamic equations predict electromagnetic waves that travel at the speed of light c that is determined by the permittivity ϵ_0 and permeability μ_0 of free space such that

$$c = 1/\sqrt{\epsilon_0\mu_0} \quad (1)$$

Thus, if these spacetime properties were independent of the motion of emitters and observers, then, the speed of light is a constant. This result was proven by the Michelson-Morley experiment in 1887. The covariance or invariance of form of Maxwell's electrodynamic equations under Lorentz transformations was shown by Lorentz and Poincaré before the formulation of special relativity. The various parameters ρ , \mathbf{J} , \mathbf{E} , and \mathbf{B} that are operated on in these equations transform in well-defined ways under Lorentz transformations such that the laws of electricity, magnetism, and electrodynamics have the same form independent of relative constant motion of observers. In 1904 [12-15], Poincaré achieved the similar covariance of the equations of Newton's laws of mechanics under Lorentz transformation of the corresponding spatial-temporal and mechanical parameters. Poincaré recognized that the inertia of material bodies would become infinite when one approached the velocity of light and predicted the relationship of matter to energy [13]:

$$E = mc^2 \quad (2)$$

In addition to its intrinsic content, the energy of an object also depends on its motion. Then, what frame is this motion relative to since there are seemingly an infinite number of possibilities, and how is this related to the acceleration of the object to acquire relative motion, the inertial mass that is accelerated, the corresponding increase in mass/energy content, and the relationship of the inertial and gravitational masses? Newton argued that it was trivial to show the necessity of an absolute frame for acceleration including rotation, but the authors of relativity could not identify absolute space. Thus, they rejected its existence and thereby rejected the basis of inertial mass, energy conservation, and the equivalence of inertial and gravitational masses as shown in this paper.

To develop an understanding of spacetime that is described by relativity and to correct its deficiencies, it is insightful to consider the history of the laws of mechanics starting with Newton. The second law is represented by

$$\mathbf{F} = \frac{d\mathbf{p}}{dt} = \frac{d(m\mathbf{v})}{dt} = m \frac{d\mathbf{v}}{dt} = m\mathbf{a} \quad (3)$$

where m is the mass of the body, \mathbf{a} is its acceleration relative to a certain frame of reference, and \mathbf{F} is the resultant force acting on the body due to all other bodies that apply the force. Newton's laws are valid in frames of reference called inertial frames, moving relative to each other with uniform velocities. Experimentally, the laws of physics are the same in all such inertial frames which provides a means to identify a frame as inertial. By this criterion, inertial frames are unaccelerating and nonrotating. Otherwise, all objects would be accelerating or rotating relative to some other frame. Such a reference frame must exist for all cases. Newton introduced the concept of absolute space to provide such an absolute frame for acceleration and rotation as well as uniform motion. According to Newton, acceleration and rotation relative to absolute space are detected by simple experiments. For example, an observer accelerated relative to the room in which he is present sees the room accelerate in the opposite direction.

Since there is no force acting on the room, the apparent acceleration is not a consequence of the Newton's second law, rather it is due to the acceleration of the observer relative to absolute space. Another example is rotation wherein the object rotating relative to absolute space can be identified by the measurement of the effect of centrifugal forces. Thus, it can be appreciated that observations consistent with physical laws permit identifying acceleration and rotation relative to absolute space, but consequences of the forces of acceleration or rotation cannot be used to determine an absolute frame for two bodies in uniform motion. Although Newton could give the criterion for absolute acceleration and absolute rotation, he could not do so for absolute velocity. Locally, motion can only be defined as relative. So, it seems impossible to define an absolute frame, and in particular, the absolute frame at rest could not be identified. Newton's absolute space was abandoned by special relativity due to this limitation of being unable to reference an inertial frame in an absolute sense. However, this inability to identify or understand the nature of absolute space and an absolute frame at rest should not be confused with the lack of their existence and the consequences for the nature of spacetime, matter, and energy.

The relativity principle is postulated on the basis of the impossibility of measuring absolute velocity. Shortcomings, problems, and paradoxes arise with special relativity. Relativity is simply a set of postulates and mathematical rules for transformation of coordinates and mechanical parameters. It provides no physical basis for the absolute loss of time in experiments such as those regarding the twin paradox even when the rulers of length, time, velocity, and kinetic energy become coincident for two inertial frames previously separated in terms of one or more of these measures. Furthermore, it provides no physical basis for the conversion of matter into energy, the equivalence of the inertial and gravitational masses, the masses of fundamental particles, and the limiting velocity c for the propagation of matter in the same sense that Maxwell's equations do for electromagnetic-waves in terms like Eq. (1). Furthermore, the basis of defining an inertial frame of reference based on relative motion ignores the kinetic energy of the objects in motion. Indeed, at each given instant, an infinite number of universes each with multi-valued total kinetic energy inventories (KEI) are predicted over the KEI range of zero to infinity. Furthermore, each member of the infinite set of "parallel" universes existing simultaneously is equally permissible.

The obvious question is how can the mass-energy of the universe be increased up to arbitrary orders of magnitude by simply selecting an inertial frame? The set of equivalent inertial frames extends over an infinite range of kinetic energies relative to even one body. For example, the mass of the universe increases by over two hundred times its rest mass corresponding to $9 \times 10^{70} J$ when comparing a frame fixed to an electron moving at $v = 0.99999c$ to one at rest with respect to the Earth-laboratory frame. Since the universe is finite and closed, and matter, energy, and spacetime are conserved, these infinite possibilities for equivalent inertial frames for the universe with their unique inventories is untenable. The frames of reference regarding relative uniform motion are only convenient means to compare measurements in those frames when absolute values are not important in the determination, and it is not necessary to determine the relative rank of the frames (e.g. the stationary versus the moving one). However, these conditions may break down, and paradoxes arise that can only be resolved by abandoning the simplified frames of special relativity and invoking an absolute frame of reference.

Specifically, in addition to the lack of energy conservation and a physical mechanism for many of its consequences, another problem that arises is the inability to determine which body is in motion when comparing relative motion in order to arrive at consistent predictions. The

limitation in uniquely and unequivocally identifying inertial frames centrally impacts the ability to interpret and apply special relativity. This is particularly acute when objects initially in the same inertial frame separate and rejoin. A famous example is the case of the twin paradox. Here two twins separate and are rejoined with intervening periods of acceleration and reversal of physical displacement. A failure of special relativity is that upon rejoining the traveling twin is younger relative to the stationary twin in contradiction to his expectations since to him, it is the stationary twin who had been in motion. Although strained “resolutions” to the asymmetrical time dilation of the traveling twin have been put forward including a far-fetched one by Einstein regarding gravitational time dilation of the general relativity theory, none are tenable [16]. The fundamental impasse is inherent in the consideration that motion is arbitrarily relative. There must be an absolute frame for each object in order to conserve the mass/energy inventory of the universe as well as resolve paradoxes such as the twin paradox.

Furthermore, relativity principle based only on frames in uniform motion excludes all of the dynamic properties of the universe. And, no two independent objects can maintain infinitely exact constant relative motion. The kinetics of matter is dynamic. Object are constantly either gaining or losing energy with changing velocities and directions, and all of the matter in the universe is accelerating as spacetime expands. The physics of essentially all forms of motion of matter including acceleration, rotation, and motion of any type in a gravitational field cannot be dealt with within the context of relative space. However, even though any motion, or parameter of inertia or electromagnetism can ultimately be measured in principle (but perhaps not always in practice) relative to absolute space as discussed in Sec I.D., a principle of relativity based on physical laws can be derived that has great utility. The principle of relativity treats relative uniform rectilinear motion, and the transforms of relativity are Lorentzian¹ and well known [17].

Resolution to the problems of special relativity as well as a physical basis for the principle of relativity derives from the physical nature of spacetime based on the absolute speed of light and absolute space determined and modified by particle production. Since the constant speed of light is the absolute limiting conversion factor from time to length, it is reasonable to expect that the laws of light propagation play a fundamental part in the definition of the properties of spacetime. Consider that the maximum speed of propagation of all fields must be the same in all inertial frames such that the law of propagation of an electromagnetic wave front in the form

$$\frac{1}{c^2} \left(\frac{\partial^2 \omega}{\partial t^2} \right) - \left[\left(\frac{\partial^2 \omega}{\partial x^2} \right) + \left(\frac{\partial^2 \omega}{\partial y^2} \right) + \left(\frac{\partial^2 \omega}{\partial z^2} \right) \right] = 0 \quad (4)$$

is of universal validity. It is appropriate to give a generalized interpretation of the law of wave front propagation and to formulate the following general postulate:

There exists a maximum speed for the propagation of any kind of action—the speed of light in free space.

This principle is very significant because the transmission of signals with greatest possible speed plays a fundamental part in the definition of concepts concerning space and time. The very notion of a definite frame of reference for describing events in space and time depends

¹ Ironically, some of the most cited experimental validations of special relativity such as the dilation of the half-life of particles such as muons moving at near light speed in cyclotrons involve constant acceleration in the storage ring rather than constant uniform rectilinear motion.

on the existence of such signals. The principle formulated above, by asserting the existence of a general upper limit for all kinds of action and signal, endows the speed of light with a universal significance, independent of the particular properties of the agency of transmission and reflecting a certain objective property of spacetime. This principle has a logical connection with the principle of relativity. For if there was no single limiting velocity, but instead different agents, e.g. light and gravitation, propagated in vacuum with different speeds, then the principle of relativity would necessarily be violated as regards at least one of the agents. The principle of the universal limiting velocity can be made mathematically precise as follows:

For any kind of wave advancing with limiting velocity and capable of transmitting signals, the equation of front propagation is the same as the equation for the front of a light wave.

Thus, the equation

$$\frac{1}{c^2} \left(\frac{\partial^2 \omega}{\partial t^2} \right) - (\text{grad}^2 \omega) = 0 \quad (5)$$

acquires a general character; it is more general than Maxwell's equations from which Maxwell originally derived it. As a consequence of the principle of the existence of a universal limiting velocity one can assert the following: the differential equations describing any field that is capable of transmitting signals must be of such a kind that the equation of their characteristics is the same as the equation for the characteristics of light waves. In addition to governing the propagation of any form of energy, the wave equation governs fundamental particles created from energy and vice versa that correspond to absolute space, the associated effects of mass on absolute spacetime, and the evolution of the universe itself. Specially, the equation that describes the electron motion given by Eq. (1.48) of Ref. [1] is the wave equation, the relativistic correction of spacetime due to particle production travels according to the wave equation, and the evolution of the universe is according to the wave equation (Eq. (49)) [18-19].

The authors of special relativity did not realize or even consider the nature of the gravitational force or the relationship between matter-energy and spacetime. Nor, did they consider the implications of relativity as a description of the physical nature of spacetime. Relativity was developed for a universe that was empty (devoid of matter and light) and infinite in extent. Yet, the universe is not only filled with matter and light, it is also dynamic in the conversion of matter to light. Furthermore, it is finite rather than infinite, and its size is also dynamic and determined by the inter-conversion of matter to energy. The physical resolution of these issues involving the nature of spacetime and the unification of all forces are achieved by applying Maxwell's equation and the generalized form of the wave equation to particle production. The solutions of the masses of fundamental particle arise naturally [20], and the evolution of the cosmos follows from the same Maxwellian equations.

Then, the relativity principle postulated on the basis of the impossibility of measuring absolute velocity is an incorrect assumption. Absolute space can be defined based on the solution of the exact conserved relationships between matter, energy, and spacetime [18]. Specifically, the production energy of each fundamental particle at rest is exact (Eqs. (32-34)), and there is a corresponding rest frame for each particle at its production. Any additional energy acquired with respect to this frame increases its inertial and gravitational mass/energy according to the Lorentz transform. Then, the production of an isolated particle from a photon of identically the production energy [18, 20] defines the absolute inertial frame at rest for the particle and

could, in principle, define absolute space that conserves the energy inventory of the universe and resolves paradoxes such as the twin paradox. The rate at which ones clock is ticking can be determined in terms of the absolute time unit defined in Sec. I.D. as the “sec” of each particle. It is possible as further discussed in Sec. I.J. to slow the clock of an object by expending energy to increase its velocity with a consequent and concomitant acceleration of the clocks of parts of the object’s surroundings such that the absolute time of the universe is conserved overall.

B. Origin of Gravity with Particle Production

Gravity is not a force separable from electromagnetism. The production of a particle having an inertial mass and a gravitational mass from a photon initially traveling at the speed of light requires time dilation and length contraction of spacetime itself as opposed to the relativistic correction of mass, length, and time of objects of inertial frames in constant relative motion. The derivation of the gravity equations and the inherent masses of particles maintains the relativity principle of Eq. (5): the constant maximum speed of light for the propagation of light and gravity wave fronts. The gravity metric corresponding to spacetime time dilation and length contraction due to the production event is derived with the boundary conditions: (i) the speed of light is constant and a maximum, (ii) the angular momentum of a photon, \hbar , is conserved, and (iii) the energy of the photon is conserved as mass. The event must be spacelike even though the photon of the particle production event travels at the speed of light and the particle must travel at a velocity less than the speed of light. The relativistically altered spacetime gives rise to a gravitational force between separated masses. Thus, the production of matter and its motion alters spacetime and the altered spacetime affects the motion of matter which must follow geodesics. The spacetime contraction and time dilation derivation based on the same principle as special relativity has a similar form as that of its Lorentz transformations relating observations from different inertial frames of reference.

C. Schwarzschild-type Space and Lorentz-type Transforms Based on the Gravitational Velocity at Particle Production

A spherically symmetrical system of mass m_0 applies to the production of a particle which implies spherical coordinates with the origin at 0. Thus, a family of curved surfaces, each with constant r , is a series of concentric spheres on which it is natural to adopt the coordinate r so that a sphere with constant r has area $4\pi r^2$, and the metric on the surface of the sphere would then be

$$ds^2 = r^2 d\theta^2 + r^2 \sin^2 \theta d\phi^2 \quad (6)$$

Such a definition of r is no longer the distance from the origin to the surface, because of the spacetime contraction caused by the mass m_0 . The form of the outgoing gravitational field front traveling at the speed of light is

$$f\left(t - \frac{r}{c}\right) \quad (7)$$

Therefore the spatial metric should be expressed as

$$ds^2 = f(r)^{-1} dr^2 + r^2 d\theta^2 + r^2 \sin^2 \theta d\phi^2 \quad (8)$$

In addition, **the existence of mass m_0 also causes time dilation and length contraction of spacetime** such that the clock on each r-sphere is no longer observed from each r-sphere to run at the same rate. That is, clocks slow down in a gravitational field [21]. Therefore, the

general form of the metric due to the relativistic effect on spacetime due to mass m_0 is

$$d\tau^2 = f(r)dt^2 - \frac{1}{c^2} \left[f(r)^{-1} dr^2 + r^2 d\theta^2 + r^2 \sin^2 \theta d\phi^2 \right] \quad (9)$$

In the case where $m_0 = 0$, space would be flat which corresponds to

$$f(r) = f(r)^{-1} = 1 \quad (10)$$

Then the spacetime metric is the Minkowski tensor. In the case that the mass m_0 is finite, the Minkowski tensor is corrected by the time dilation and length contraction of spacetime.

The photon initially traveling at the speed of light undergoes particle production and must produce a gravitational field that travels at the speed of light. According to Newton's Law of Gravitation, the particle must have a finite velocity relative to the antiparticle called the Newtonian gravitational velocity, v_g , (Eq. (15)) that may not exceed the speed of light and has an associated gravitational energy given previously [18]. The eccentricity is one, the total energy is zero, and the particle production trajectory is a parabola relative to the center of mass of the antiparticle [18]. In order that the velocity of light does not exceed c in any frame including that of the particle having a finite Newtonian gravitational velocity, v_g , the laboratory frame of an incident photon, and that of a gravitational field propagating outward at the speed of light, spacetime must undergo time dilation and length contraction due to the production event. During particle production the speed of light as a constant maximum as well as phase matching and continuity conditions require the following form of the squared displacements due to constant motion along two orthogonal axes in polar coordinates:

$$(c\tau)^2 + (v_g t)^2 = (ct)^2 \quad (11)$$

$$\tau^2 = t^2 \left(1 - \left(\frac{v_g}{c} \right)^2 \right) \quad (12)$$

Thus,

$$f(r) = \left(1 - \left(\frac{v_g}{c} \right)^2 \right) \quad (13)$$

The derivation and result of spacetime time dilation is analogous to the derivation and result of special relativistic time dilation wherein the gravitational velocity replaces the relative velocity of two inertial frames in the Lorentz factor β . The general form of the metric due to the relativistic effect on spacetime due to mass m_0 is

$$d\tau^2 = \left(1 - \left(\frac{v_g}{c} \right)^2 \right) dt^2 - \frac{1}{c^2} \left[\left(1 - \left(\frac{v_g}{c} \right)^2 \right)^{-1} dr^2 + r^2 d\theta^2 + r^2 \sin^2 \theta d\phi^2 \right] \quad (14)$$

The equivalence of the gravitational and inertial masses according to experiments and Eqs. (34) and (53-55) prove that Newton's Gravitational Law is exact on a local scale. The correction to Newton's Gravitational Law due to the relativistic effect of the presence of mass on spacetime may be determined by substitution of the gravitational escape velocity, v_g , given by

$$v_g = \sqrt{\frac{2Gm_0}{r}} = \sqrt{\frac{2Gm_0}{\tilde{\lambda}_c}} \quad (15)$$

into Eq.(14) for v_g . The corresponding Newtonian gravitational radius is given by [22]

$$r_g = \frac{2Gm_0}{c^2} \quad (16)$$

Thus, Eq. (14) can also be expressed as

$$d\tau^2 = \left(1 - \frac{r_g}{r}\right) dt^2 - \frac{1}{c^2} \left[\left(1 - \frac{r_g}{r}\right)^{-1} dr^2 + r^2 d\theta^2 + r^2 \sin^2 \theta d\phi^2 \right] \quad (17)$$

In the case of the boundary conditions of Eqs. (33-34), Eq. (15) and Eq. (16), three families of leptons and quarks are predicted [20] wherein each particle corresponds to a unique particle-production radius equal to its Compton wavelength bar. At particle production, a photon having a radius and a wavelength equal to the Compton wavelength bar of the particle forms a transition state of the particle of the same wavelength.

$$r = \tilde{\lambda}_C = \frac{\hbar}{mc} = r_\alpha^* \quad (18)$$

The resulting metric $g_{\mu\nu}$ for non-Euclidean space due to the relativistic effect on spacetime due to mass m_0 with v_g given by Eq. (15) is

$$g_{\mu\nu} = \begin{pmatrix} -\left(1 - \frac{2Gm_0}{c^2 r}\right) & 0 & 0 & 0 \\ 0 & \frac{1}{c^2} \left(1 - \frac{2Gm_0}{c^2 r}\right)^{-1} & 0 & 0 \\ 0 & 0 & \frac{1}{c^2} r^2 & 0 \\ 0 & 0 & 0 & \frac{1}{c^2} r^2 \sin^2 \theta \end{pmatrix} \quad (19)$$

In this case, the separation of proper time between two events x^μ and $x^\mu + dx^\mu$ is

$$d\tau^2 = \left(1 - \frac{2Gm_0}{c^2 r}\right) dt^2 - \frac{1}{c^2} \left[\left(1 - \frac{2Gm_0}{c^2 r}\right)^{-1} dr^2 + r^2 d\theta^2 + r^2 \sin^2 \theta d\phi^2 \right] \quad (20)$$

The *Schwarzschild-type metric* (Eq. (20)) gives the relationship whereby matter causes relativistic corrections to spacetime that determines the curvature of spacetime and is the origin of gravity.

The origin of gravity is fundamental particles, and the masses and fields from particles superimpose. So, m_0 , the mass of a fundamental particle, may be replaced by M , the sum of the masses of the particles which make up a massive body. In this case, Eq. (20) is equivalent to a modified version of the Schwarzschild-type metric that is conservative of matter, energy, and spacetime and lacking the reduced radial coordinate, $r - \frac{GM}{c^2}$, and singularity issues of general relativity.

The Schwarzschild-type metric provides transforms of the spacetime and mass-energy parameters based on the effect of gravity in an analogous manner as the Minkowski tensor

provides the Lorentz transforms for the corresponding inertial parameters. As shown in Eq. (32.70) of Ref. [1], the relativistic correction for time is

$$t = \frac{\tau}{\sqrt{1 - \frac{v_g^2}{c^2}}} \quad (21)$$

Then,

$$l = l_o \sqrt{1 - \frac{v_g^2}{c^2}} \quad (22)$$

The spacetime corrections have the same form as the special relativistic corrections for time and length with v_g in place of v . Consider the relationship between proper and coordinate mass derived previously [18] by considering an object of mass m orbiting an object of mass M . The gravitational force is central; thus the angular momentum is constant. Consider that a radial force is applied to increase the radius r of the object's orbit with a change of its energy E . The angular momentum is conserved; thus,

$$mr_i^2 \left(\frac{d\phi}{dt} \right)_i = mr_f^2 \left(\frac{d\phi}{dt} \right)_f \quad (23)$$

where $\left(\frac{d\phi}{dt} \right)_i$ is the initial angular velocity, $\left(\frac{d\phi}{dt} \right)_f$ is the final angular velocity, r_i is the initial radius and r_f is the final radius. At fixed radius, dr^2 is zero, but dt^2 is finite. Applying the time relativistic correction given by Eq. (20) and Eqs. (11-13) gives the mass m_f at r_f with respect to the mass m_i of the inertial frame of r_i as

$$m_i \sqrt{\left(1 - \frac{2GM}{rc^2} \right)} = m_f \quad (24)$$

where r is the increase in the radius. The proper energy E_p of the object is given by

$$m_i c^2 \sqrt{\left(1 - \frac{2GM}{rc^2} \right)} = E_p \quad (25)$$

The relativistic correction for energy is of the same form as the special relativistic correction for mass with v_g in place of v :

$$\frac{E}{\sqrt{1 - \left(\frac{v_g}{c} \right)^2}} = mc^2 \quad (26)$$

where m is the coordinate mass of the orbiting body and E is the energy of the orbiting object. In the case that the gravitational velocity is much less than the speed of light ($v_g \ll c$), the gravitational energy E_g converges to that given by Newton's law of Gravitation.

$$E \approx mc^2 \left(1 - \frac{1}{2} \left(\frac{2GM}{rc^2} \right) \right) \quad (27)$$

$$E \approx mc^2 - \frac{GMm}{r} \quad (28)$$

$$E_g = -\frac{GMm}{r} \quad (29)$$

D. Particle Production Continuity Conditions from Maxwell's Equations, and the Schwarzschild-type Metric Give Rise to Charge, Momentum, and Mass

The photon possesses electric and magnetic fields and the corresponding energies and momentum. The angular momentum of the photon given by [23]

$$\mathbf{m} = \int \frac{1}{8\pi c} \text{Re}[\mathbf{r} \times (\mathbf{E} \times \mathbf{B}^*)] dx^4 = \hbar \quad (30)$$

is conserved [24] during particle production. The energy due to the angular frequency of the photon according to Planck's equation and those of its electric and magnetic fields match those of the particle to which it gives rise. The transition state has dimensions of the particle's Compton wavelength bar such that the speed matches light speed at the photon's frequency as a further constraint of Maxwell's equations and the inherent special relativity. This limiting speed is set by the permittivity and permeability of spacetime. Spacetime undergoes time dilation and length contraction at the particle production event as a gravitation-field front propagates out as a light-wave front at light speed. The photon's effect on spacetime and spacetime's effect on the corresponding production particle then determine its inertial and gravitational mass m_0 and the fundamental charge e where the momentum and energies of the photon are continuous with those of the particle during the production event.

The photon to particle event requires a transition state that is continuous wherein the intrinsic velocity of the transition state is the speed of light [18]. The radius, r , is the Compton wavelength bar, $\tilde{\lambda}_c$, given by Eq. (18). At production, the Planck equation energy, the electric potential energy, and the magnetic energy are equal to m_0c^2 [18].

The Schwarzschild-type metric gives the relationship whereby matter causes relativistic corrections to spacetime that determines the masses of fundamental particles. Substitution of $r = \tilde{\lambda}_c$; $dr = 0$; $d\theta = 0$; $\sin^2 \theta = 1$ into the Schwarzschild-type metric gives

$$d\tau = dt \left(1 - \frac{2Gm_0}{c^2 r_\alpha^*} - \frac{v^2}{c^2} \right)^{\frac{1}{2}} \quad (31)$$

with $v^2 = c^2$, the relationship between the proper time and the coordinate time is

$$\tau = ti \sqrt{\frac{2GM}{c^2 r_\alpha^*}} = ti \sqrt{\frac{2GM}{c^2 \tilde{\lambda}_c}} = ti \frac{v_g}{c} \quad (32)$$

When the intrinsic particle velocity is the speed of light, continuity conditions based on the constant maximum speed of light given by Maxwell's equations are mass energy = Planck equation energy = electric potential energy = magnetic energy = mass/spacetime metric energy. Therefore,

$$m_0c^2 = \hbar\omega^* = V = E_{\text{mag}} = E_{\text{spacetime}} \quad (33)$$

$$m_0c^2 = \hbar\omega^* = \frac{\hbar^2}{m_0\tilde{\lambda}_c^2} = \alpha^{-1} \frac{e^2}{4\pi\epsilon_0\tilde{\lambda}_c} = \alpha^{-1} \frac{\pi\mu_0 e^2 \hbar^2}{(2\pi m_0)^2 \tilde{\lambda}_c^3} = \frac{\alpha h}{1 \text{ sec}} \sqrt{\tilde{\lambda}_c c^2} \quad (34)$$

The continuity conditions based on the constant maximum speed of light given by the Schwarzschild-type metric are:

$$\frac{\text{proper time}}{\text{coordinate time}} = \frac{\text{gravitational wave condition}}{\text{electromagnetic wave condition}} = \frac{\text{gravitational mass phase matching}}{\text{charge/inertial mass phase matching}}$$

$$\frac{\text{proper time}}{\text{coordinate time}} = i \frac{\sqrt{\frac{2Gm}{c^2 \lambda_c}}}{\alpha} = i \frac{v_g}{\alpha c} \quad (35)$$

Each of the Planck equation energy, electric energy, and magnetic energy corresponds to a particle given by the relationship between the proper time and the coordinate time [20]. The electron and down-down-up neutron correspond to the Planck equation energy. The muon and strange-strange-charmed neutron correspond to the electric energy. The tau and bottom-bottom-top neutron correspond to the magnetic energy. The particle must possess the escape velocity v_g relative to the antiparticle where $v_g < c$. According to Newton's law of gravitation, the eccentricity is one and the particle production trajectory is a parabola relative to the center of mass of the antiparticle. The masses of the three families of leptons and quarks are given in Ref. [20]. Exemplary relations between fundamental particles are shown in Table 1.

Consider pair production. The proper time of the particle is equated with the coordinate time according to the Schwarzschild-type metric corresponding to light speed. The special relativistic condition corresponding to the Planck energy (Eq. (34)) gives the mass of the electron [25-26]:

$$2\pi \frac{\hbar}{mc^2} = \sec \sqrt{\frac{2Gm^2}{c\alpha^2 \hbar}} \quad (36)$$

$$m_e = \left(\frac{h\alpha}{\sec c^2} \right)^{\frac{1}{2}} \left(\frac{c\hbar}{2G} \right)^{\frac{1}{4}} = 9.0998 \times 10^{-31} \text{ kg} \quad (37)$$

where $m_{e \text{ experimental}} = 9.10945455 \times 10^{-31} \text{ kg}$. A clock is defined in terms of a self-consistent system of units used to measure the particle mass. Presently the second is defined as the time required for 9,192,631,770 vibrations within the cesium-133 atom. The "sec" as defined in Eqs. (34) and (36) is a fundamental constant, namely, the metric of spacetime (it is almost identically equal to the present value of the MKS second as explained previously [18]). A unified theory can only provide the relationships between all measurable observables in terms of a clock defined in terms of fundamental constants according to those observables and used to measure them. The so defined "clock" measures "clicks" on an observable in one aspect, and in another, it is the ruler of spacetime of the universe with the implicit dependence of spacetime on matter-energy conversion as shown previously [27]. The production of an isolated particle from a photon of identically the production energy defines the absolute inertial frame at rest for the particle and could, in principle, define absolute space that conserves the energy inventory of the universe and resolves paradoxes such as the twin paradox. The rate at which ones clock is ticking can be determined in terms of the absolute time unit defined as the "sec" of each particle.

E. Relationship of Matter to Energy and Spacetime Expansion

The Schwarzschild-type metric gives the relationship whereby matter causes relativistic corrections to spacetime. The limiting velocity c results in the contraction of spacetime due to particle production, which is given by $2\pi r_g$ where r_g is the gravitational radius of the particle. This has implications for the expansion of spacetime when matter converts to energy. Q the mass/energy to expansion/contraction quotient of spacetime is given by the ratio of the mass of a particle at production divided by T , the period of production [18].

$$Q = \frac{m_0}{T} = \frac{m_0}{\frac{2\pi r_g}{c}} = \frac{m_0}{2\pi \frac{2Gm_0}{c^2}} = \frac{c^3}{4\pi G} = 3.22 \times 10^{34} \frac{kg}{sec} \quad (38)$$

The gravitational equations with the equivalence of the particle production energies (Eq. (34)) permit the conservation of mass/energy ($E = mc^2$) and spacetime ($\frac{c^3}{4\pi G} = 3.22 \times 10^{34} \frac{kg}{sec}$).

With the conversion of $3.22 \times 10^{34} \text{ kg}$ of matter to energy, spacetime expands by 1 sec. The photon has inertial mass and angular momentum, but due to Maxwell's equations and the implicit special relativity it does not have a gravitational mass. The observed gravitational deflection of light is predicted [18].

F. Cosmological Consequences

The Universe is closed (it is finite but with no boundary). It is a 3-sphere Universe-Riemannian three dimensional hyperspace plus time of constant positive curvature at each r-sphere. *The Universe is oscillatory in matter/energy and spacetime* with a finite minimum radius, the gravitational radius. Spacetime expands as mass is released as energy which provides the basis of the *atomic, thermodynamic, and cosmological arrows of time*. Different regions of space are isothermal even though they are separated by greater distances than that over which light could travel during the time of the expansion of the Universe [28]. Presently, stars and large scale structures exist which are older than the elapsed time of the present expansion as stellar, galaxy, and supercluster evolution occurred during the contraction phase [29–35]. The maximum power radiated by the Universe which occurs at the beginning of the expansion phase is $P_U = \frac{c^5}{4\pi G} = 2.89 \times 10^{51} \text{ W}$. Observations beyond the beginning of the expansion phase are not possible since the Universe was entirely matter filled.

G. The Period of Oscillation of the Universe Based on the Closed Propagation of Light

Mass/energy is conserved during harmonic expansion and contraction. The gravitational potential energy E_{grav} with $m_0 = m_U$ is equal to $m_U c^2$ when the radius of the Universe r is the gravitational radius r_G ($r_G = \frac{Gm_0}{c^2}$). The gravitational velocity v_G ($v_G = \sqrt{\frac{Gm_0}{r}} = \sqrt{\frac{Gm_0}{\lambda_c}}$) with $r = r_G$ and $m_0 = m_U$ is the speed of light in a circular orbit wherein the eccentricity is equal to zero and the escape velocity from the Universe can never be reached. The period of the

oscillation of the Universe and the period for light to transverse the Universe corresponding to the gravitational radius r_G must be equal. The harmonic oscillation period, T , is

$$T = \frac{2\pi r_G}{c} = \frac{2\pi G m_U}{c^3} = \frac{2\pi G (2 \times 10^{54} \text{ kg})}{c^3} \quad (39)$$

$$= 3.10 \times 10^{19} \text{ sec} = 9.83 \times 10^{11} \text{ years}$$

where the mass of the Universe, m_U , is approximately $2 \times 10^{54} \text{ kg}$. Thus, the observed Universe will expand as mass is released as photons for $4.92 \times 10^{11} \text{ years}$. At this point in its world line, the Universe will obtain its maximum size and begin to contract.

H. The Differential Equation of the Radius of the Universe

Based on conservation of mass/energy ($E = mc^2$) and spacetime ($\frac{c^3}{4\pi G} = 3.22 \times 10^{34} \frac{\text{kg}}{\text{sec}}$), the Universe behaves as a simple harmonic oscillator having a restoring force, \mathbf{F} , which is proportional to the radius. The proportionality constant, k , is given in terms of the potential energy, E , gained as the radius decreases from the maximum expansion to the minimum contraction.

$$\frac{E}{\aleph^2} = k \quad (40)$$

Since the gravitational potential energy E_{grav} is equal to $m_U c^2$ when the radius of the Universe r is the gravitational radius r_G

$$F = -k\aleph = -\frac{m_U c^2}{r_G^2} \aleph = -\frac{m_U c^2}{\left(\frac{G m_U}{c^2}\right)^2} \aleph \quad (41)$$

and, considering the oscillation, the differential equation of the radius of the Universe, \aleph is

$$m_U \ddot{\aleph} + \frac{m_U c^2}{r_G^2} \aleph = m_U \ddot{\aleph} + \frac{m_U c^2}{\left(\frac{G m_U}{c^2}\right)^2} \aleph = 0 \quad (42)$$

The *maximum radius of the Universe*, the amplitude, r_0 , of the time harmonic variation in the radius of the Universe, is given by the quotient of the total mass of the Universe and Q (Eq. (38)), the mass/energy to expansion/contraction quotient:

$$r_0 = \frac{m_U}{Q} = \frac{m_U}{\frac{c^3}{4\pi G}} = \frac{2 \times 10^{54} \text{ kg}}{\frac{c^3}{4\pi G}} = 1.97 \times 10^{12} \text{ light years} \quad (43)$$

The *minimum radius* which corresponds to the gravitational radius, r_g , given by Eq. (16) with $m_0 = m_U$ is

$$r_g = \frac{2G m_U}{c^2} = 2.96 \times 10^{27} \text{ m} = 3.12 \times 10^{11} \text{ light years} \quad (44)$$

When the radius of the Universe is the gravitational radius, r_g , the proper time is equal to the coordinate time by Eq. (32), and the gravitational escape velocity v_g of the Universe is the speed of light. The radius of the Universe as a function of time is

$$\aleph = \left(r_g + \frac{cm_U}{Q} \right) - \frac{cm_U}{Q} \cos \left(\frac{2\pi t}{\frac{2\pi r_G}{c}} \right) = \left(\frac{2Gm_U}{c^2} + \frac{cm_U}{\frac{c^3}{4\pi G}} \right) - \frac{cm_U}{\frac{c^3}{4\pi G}} \cos \left(\frac{2\pi t}{\frac{2\pi Gm_U}{c^3}} \right) \quad (45)$$

As in Ref. [18], Eq. (45) correctly predicts the observed size, age, Hubble constant, temperature, density of matter, power spectrum, large-scale structure, and *acceleration rate of the expansion of the universe*. The latter astonishing observation was predicted years before it was observed [36].

I. The Periods of Spacetime Expansion/Contraction and Particle Decay/Production for the Universe are Equal

The period of the expansion/contraction cycle of the radius of the Universe, T , is given by Eq. (39). It follows from the Poynting power theorem with spherical radiation that the transition lifetimes are given by the ratio of energy and the power of the transition. Exponential decay applies to electromagnetic energy decay:

$$h(t) = e^{-\alpha t} u(t) = e^{-\frac{2\pi}{T} t} u(t) \quad (46)$$

The coordinate time is imaginary because energy transitions are spacelike due spacetime expansion from matter to energy conversion. For example, the mass of the electron (a fundamental particle) is given by

$$\frac{2\pi \tilde{\lambda}_c}{\sqrt{\frac{2Gm_e}{\tilde{\lambda}_c}}} = \frac{2\pi \tilde{\lambda}_c}{v_g} = i\alpha^{-1} \text{ sec} \quad (47)$$

where v_g is Newtonian gravitational velocity (Eq. (15)). When the gravitational radius r_g is the radius of the Universe, the proper time is equal to the coordinate time by Eq. (32), and the gravitational escape velocity v_g of the Universe is the speed of light. Replacement of the coordinate time, t , by the spacelike time, it , gives

$$h(t) = \text{Re} \left[e^{-\frac{2\pi}{T} it} \right] = \cos \frac{2\pi}{T} t \quad (48)$$

where the period is T (Eq. (39)). The continuity conditions based on the constant maximum speed of light (Maxwell's equations) are given by Eqs. (33-34). The continuity conditions based on the constant maximum speed of light (Schwarzschild-type metric) are given by Eq. (35). The periods of spacetime expansion/contraction and particle decay/production for the Universe are equal because only the particles which satisfy Maxwell's equations and the relationship between proper time and coordinate time imposed by the Schwarzschild-type metric may exist.

The general form of the light front wave equation is given by Eq. (4). The equation of the radius of the Universe, \aleph , may be written as

$$\aleph = \left(\frac{2Gm_U}{c^2} + \frac{cm_U}{c^3} \right) - \frac{cm_U}{c^3} \cos \left(\frac{2\pi}{2\pi Gm_U} \left(t - \frac{\aleph}{c} \right) \right) \quad (49)$$

which is a solution of the wave equation for a light wave front. Maxwell's equations, Planck's equation, the de Broglie equation, Newton's laws, and special relativity, and gravity are unified. Classical physical laws apply on all scales wherein space is finite-absolute rather than infinite-relative.

J. Equivalence of the Gravitational and Inertial Masses

The relationships of relativity and gravity have the same form with the interchange of the inertial and gravitational velocities. The relationships are reciprocal due to the nature of absolute space that is produced or annihilated with particle annihilation or production, respectively. Due to the finite propagation time for signals set by the speed of light which is in turn set by the finite permeability and permittivity of free space, the mechanics parameters are corrected by Lorentz transformations or their equivalent with the gravitational velocity replacing the constant kinetic velocity in the case of gravitating bodies.

Extensive experimentation dating from Galileo Galilei's Pisa experiment to the present has shown that irrespective of the object chosen, the acceleration of an object produced by the gravitational force is the same, which from

$$a = \frac{m_g}{m_i} \left(\frac{GM_{\oplus}}{r^2} \right) \quad (50)$$

implies that the value of m_g / m_i should be the same for all objects. In other words, we have

$$\frac{m_g}{m_i} = \text{universal constant} \quad (51)$$

the equivalence of the gravitational mass and the inertial mass. The fractional deviation of Eq. (51) from a constant is experimentally confirmed to less 1×10^{-11} [37]. The equivalence of the gravitational mass and the inertial mass is a conservation statement of the mass, energy, and spacetime of the universe. The overall inventory is a constant with the inter-conversion related by the ratios of fundamental constants of spacetime (Eqs. (33-34)).

At particle production, the outgoing gravitational field, traveling as a wave front, carries the change in the curvature of spacetime. The front must travel at light speed since the permittivity ϵ_0 and permeability μ_0 of free spacetime are and must remain independent of curvature in order for the laws of physics to be covariant and the physics of the universe to be conservative. Thus, any perturbation must travel at the speed of light c given by Eq. (1). The justification for Eq. (11) is the relativity principle based on Eq. (5) and the invariance of the light speed due to the invariance of the permittivity ϵ_0 and permeability μ_0 of free spacetime.

From Eqs. (20) and (32-38), each r-sphere of the universe comprising a finite, closed 3-sphere universe-(Riemannian three-dimensional hyperspace plus time of constant positive curvature at each r-sphere) is determined by a clock set by the conservation relationship of mass-

energy, $E = mc^2$, and spacetime, $\frac{c^3}{4\pi G} = 3.22 \times 10^{34} \frac{kg}{sec}$. Spacetime expands at light speed as

mass is released as energy which provides the basis of the atomic, thermodynamic, and

cosmological arrows of time.

Consider the relationship (Eq. (26)) between gravitational mass m_g and proper energy E_p of a gravitating object based on the absolute light speed and absolute space:

$$\frac{E_p}{\sqrt{1 - \left(\frac{v_g}{c}\right)^2}} = m_g c^2 \quad (52)$$

Similarly, based on the absolute light speed and absolute space, the relationship between inertial mass m_i and energy is

$$E_p = m_i c^2 = \frac{m_0 c^2}{\sqrt{1 - \frac{v^2}{c^2}}} \quad (53)$$

At particle production, $v = v_g$ and Eqs. (32-34) are continuously satisfied with a final free state at rest, such that

$$E_p = m_g c^2 \sqrt{1 - \left(\frac{v_g}{c}\right)^2} = m_i c^2 \sqrt{1 - \frac{v^2}{c^2}} = m_0 c^2 \quad (54)$$

Thus,

$$m_g = m_i = m_0 \quad (55)$$

wherein a particle's absolute frame of reference is determined by the production event having production mass m_0 (e.g. Eq. (37)), energy $m_0 c^2$ (Eq. (34)), velocity v_g (Eq. (15)) in the photon-particle transition state and zero as a free particle, and the proper time defined in terms of the unit *sec* of its proper clock which depends on its gravitational and inertial masses (Eqs. (32), (34), (36)) which are equivalent. Following production, conservation of mass-energy relative to absolute space and consequently relative space in Eqs. (53) and (26) requires that

$$m_g = m_i \quad (56)$$

where the energy is a Lorentz scalar and the contributions due to kinetic energy and gravitational energy corresponding to v and v_g , respectively, superimpose. The validity of the gravity metric under interchange of the masses of gravitating bodies requires that Eqs. (55-56) apply in general.

The absolute gravitational and inertial masses are equivalent since they both obey the relativity principle and conservation of mass-energy-spacetime. With regard to gravitational effects, clocks and rulers are affected by the acquisition of translational velocity. The gravitational mass increases by the kinetic energy increase. This causes a gravitating particle's internal clock to undergo gravitational dilation such that its proper time with respect to the absolute time unit *sec* is synchronized with the mass-energy expansion-contraction cycle of the universe. Since the same physical relationships hold for all frames of reference (Relativity Principle), the relative inertial and gravitational masses are equivalent in their effects from the perspective of the corresponding frames. This result also provides a gravitational causality constraint regarding the maximum particle speed that matches that imposed by the particle's equivalent gravitational and inertial masses. In addition to the impossible result that the inertia of the particle would become infinite when it approached the velocity of light as first recognized by Poincaré [12], the principle that the particle velocity cannot exceed c also arises from the

existence of absolute space. A particle's gravitational mass cannot become infinite, and the particle's position cannot outdistance the spacetime perturbation created by its production or any mass increase from the acquisition of kinetic energy.

Regarding the inertial implications, based on the absolute speed of light, measurements by clocks in different inertial frames deviate in a manner independent of that due to spacetime curvature caused by gravitating bodies. These effects are also due to an absolute change in the particle's mass-energy-spacetime parameters. They are not due to different relative perceptions of time measurement as inherent in the current interpretations of special relativity. For example, the appearance that a stick immersed in water appears to bend can be understood in terms of the difference in the speed of light propagation in air and water. The molecules are not really forming new bonds. But, clocks that were initially synchronized and at relative rest, have undergone relative translation, and were rejoined, measure different times in an absolute sense, not just a relative one. And, thereafter the relative velocity is zero, the increase in kinetic energy has gone to zero, and any contraction of physical dimensions due to relativity is not observed. Time has been absolutely lost due to motion. This conclusion is in agreement with the results of the twin paradox and differences in the observation of the simultaneity of events due to motion. It is possible to slow the clock of an object by expending energy to increase its velocity with a consequent and concomitant acceleration of the clocks of parts of the object's surroundings such that the absolute time of the universe is conserved overall. As shown in Secs. I. E and I.F. spacetime expands as mass is released as energy which provides the basis of the *atomic, thermodynamic, and cosmological arrows of time*. The resulting object's kinetic energy is also an absolute as opposed to a relative parameter. It represents a conservative physical change in the mass-energy-spacetime inventory of the universe. It can be quantified in terms of absolutes with the inertial and gravitational masses being equivalent as a requirement of the conservation of mass, energy, and spacetime.

The equivalence of the inertial and gravitational masses is due to mass-energy conservation relative to absolute space whose permittivity and permeability and gravitational constant determine the conversion factor between mass and energy and the mass and curvature, respectively. Since the gravitational and inertial mass are equivalent, the same mass value for a gravitating body with inertia is used in both the gravitational and inertial equations of motion. Given that a particle's mass is absolute relative to absolute space according to

$$m = \frac{m_0}{\sqrt{1 - \frac{v^2}{c^2}}} \quad (57)$$

wherein v is the absolute velocity, the factor of resistance to any change in velocity due to an applied force corresponding to a change in kinetic energy and therefore mass-energy inventory over space and time is the inertial mass. Thus, conservation of mass-energy when there is any change is the basis of an absolute law, namely Newton's second law.

K. Newton's Second Law

The basis of the equivalence of inertial and gravitational mass of fundamental particles is inherent in the particle production event that additionally requires that spacetime is absolute and Riemannian due to a relativistic correction to spacetime with particle production [18, 38]. Thus, inertial mass is none other than an expression of the absolute energy inventory of a particle relative to absolute space and Newton's second law is just the differential form of this fact. Thus, Newton's force law can be derived from these relationships:

$$\begin{aligned}
F &= \frac{dE}{ds} = \frac{d(mc^2)}{ds} = \frac{d\left(\frac{m_0 c^2}{\sqrt{1-\frac{v^2}{c^2}}}\right)}{ds} = \frac{1}{2} \frac{m_0 c^2}{\left(1-\frac{v^2}{c^2}\right)^{3/2}} \frac{2v}{c^2} \frac{dv}{ds} = \frac{1}{2} \frac{m_0 c^2}{\left(1-\frac{v^2}{c^2}\right)^{3/2}} \frac{2}{c^2} \frac{ds}{dt} \frac{dv}{ds} \\
&= \frac{m_0}{\left(1-\frac{v^2}{c^2}\right)^{3/2}} \frac{dv}{dt}
\end{aligned} \tag{58}$$

Considering the invariant momentum, the time derivative is given by

$$\frac{dp}{dt} = \frac{d}{dt} \left(\frac{m_0 v}{\sqrt{1-\frac{v^2}{c^2}}} \right) = \frac{m_0}{\left(1-\frac{v^2}{c^2}\right)^{3/2}} \frac{dv}{dt} \tag{59}$$

Comparison of Eq. (58) with Eq. (59) gives Newton's force law (Eq. (3)):

$$F = \frac{d}{dt} \left(\frac{m_0 v}{\sqrt{1-\frac{v^2}{c^2}}} \right) = \frac{d\mathbf{p}}{dt} \tag{60}$$

Thus, the application of a force causes acceleration relative to absolute space to a new final absolute velocity corresponding to the final absolute mass where the mass difference is the increased kinetic energy. Since the absolute-mass-energy of the source of force decreases exactly by that amount by which the accelerated body increases, the mass-energy inventory of the universe is conserved. Newton's second law is equivalent to conservation of energy.

L. Fifth Force

The relationship between inertial and gravitational mass is based on the result that only fundamental particles having an equivalence of the inertial and gravitational masses at particle production are permitted to exist since only in these cases are Maxwell's equations and the conditions inherent in the Schwarzschild-type metric of spacetime satisfied simultaneously wherein space must be absolute. The equivalence is maintained for any velocity thereafter due to the absolute nature of space and the absolute speed of light. The invariant speed c is set by the permittivity and permeability of absolute space that determines the relativity principle based on propagation of fields and signals as light-wave fronts. The predicted twin-paradox result based on Poincaré's postulates, Lorentz transforms, and absolute space has been verified by experiments in which extremely precise and accurate clocks are synchronized, divided into identical Earth-bound and traveling clocks, and the times of stationary members are compared with ones flown around the world on airplanes [39].

Now knowing the nature of spacetime and its relationship to the inertial and gravitational masses of fundamental particles, *consider the possibility of using these relationships to break the equivalence of the inertial and gravitational masses.* In light of past conceptions, such a nonequivalence is an impossibility. In Einstein's gravity equation, the Einstein's Tensor $G_{\mu\nu}$, is equal to the stress-energy-momentum tensor $T_{\mu\nu}$. This equation does not consider the constant maximum speed of light at particle production or any other physical constraint with particle

production and the corresponding implications for gravity, and incorrectly postulates the equality of the photon energy to a mass according to Eq. (53). Since it is merely postulated based on the disproved Equivalence Principle (equivalence of an accelerating inertial frame and a gravitational field), it is not surprising that it is not predictive. For example, it does not predict the inertial or gravitational masses of particles wherein the latter is the origin of gravity. Furthermore, it gives rise to incorrect predictions, the most recent failure being that all solutions predict a decelerating cosmology in disagreement with the observed acceleration of the expansion [40, 41]. Furthermore, the only possibility is for the gravitational mass to be equivalent to the inertial mass. A particle of zero or negative gravitational mass is not possible. However, the correct basis of gravitation is not according to Einstein's equation; instead, the origin of gravity is the relativistic correction of spacetime itself which is analogous to the special relativistic corrections of inertial parameters—increase in mass, dilation in time, and contraction in length in the direction of constant relative motion of separate inertial frames. On this basis, the observed acceleration of the cosmos was predicted [18, 36] using the same equations that predict the masses of fundamental particles including that of the top quark before it was observed. The physical solution of the spacetime metric also predicts the previously observed zero gravitational mass of the photon [18] and free electron [42]. Furthermore, it makes the fundamental prediction, that is experimentally confirmed in this paper, of the existence of a fifth force in the opposite direction and of much greater magnitude than the gravitational force.

The Schwarzschild-type metric gives the relationship whereby matter causes relativistic corrections to spacetime that determines the curvature of spacetime and is the origin of gravity. The relationship of matter and spacetime then has implications for the motion of matter relative to a gravitating body based on its intrinsic motion. Matter arises during particle production from a photon and comprises mass and charge confined to a two-dimensional surface based on the derivation of the structure of fundamental particles given previously [1, 43]. Matter of fundamental particles such as an electron has zero thickness. But, in order that the speed of light is a constant maximum in any frame including that of the gravitational field that propagates out as a light-wave front at particle production, the production event gives rise to a spacetime dilation equal to 2π times the Newtonian gravitational or Schwarzschild radius

$$r_g = \frac{2Gm_e}{c^2} = 1.3525 \times 10^{-57} \text{ m} \text{ of the particle according to Eqs. (16) and (38) in details given in}$$

Ref. [18]. For the electron, this corresponds to a spacetime dilation of $8.4980 \times 10^{-57} \text{ m}$ or $2.8346 \times 10^{-65} \text{ s}$. Although the electron does not occupy space in the third spatial dimension, its mass discontinuity effectively "displaces" spacetime wherein the spacetime dilation can be considered a "thickness" associated with its gravitational field. Matter and the motion of matter effects the curvature of spacetime which in turn influences the motion of matter. Consider the angular motion of matter of a fundamental particle. The angular momentum of the photon is \hbar . An electron is formed from a photon, and it can only change its bound states in discrete quantized steps caused by a photon at each step. Thus, the electron angular momentum is always quantized in terms of \hbar . But, this intrinsic motion comprises a two-dimensional velocity surface of the motion of the matter through space that may be positively curved, flat, or negatively curved. The first case corresponds to the bound electron having the equivalence of the gravitational and inertial masses. The second case corresponds to the free electron having an experimentally measured deviation between the inertial and gravitational masses. The experimental mass of the free electron measured by Witteborn [42] using a free fall technique is

less than $0.09 m_e$, where m_e is the inertial mass of the free electron ($9.109534 \times 10^{-31} \text{ kg}$). Thus, a free electron is not gravitationally attracted to ordinary matter, and the gravitational and inertial masses are not equivalent. The third case corresponds to an extraordinary state of matter called a **hyperbolic electron** given in Sec. I.M. Due to interplay between the motion of matter and spacetime in terms of their respective geometries, only in the first case is the inertial and gravitational masses of the electron equivalent. In the second case, the gravitational mass is zero, and in the third case, the gravitational mass is negative in the equations of extrinsic or translational motion. The negative gravitational mass of a fundamental particle is the basis of and is manifested as a **fifth force** that acts on the fundamental particle in the presence of a gravitating body in a direction opposite to that of the gravitational force with far greater magnitude.

The relativistic correction for spacetime dilation and contraction due to the production of a particle with positive curvature is given by Eq. (13). The derivation of the relativistic correction factor of spacetime was based on the constant maximum velocity of light and a finite positive Newtonian gravitational velocity v_g of the particle given by Eq. (15). Using v_g and the Newtonian gravitational radius, r_g , of each particle at the production event, each of mass m_0 given by Eq. (16), the Schwarzschild-type metric for bound matter is given by Eqs. (14) and (17), respectively. The solutions for the Schwarzschild-type metric exist wherein the relativistic correction to the gravitational velocity v_g and the gravitational radius r_g are of the opposite sign (i.e. negative). In these cases, the Schwarzschild-type metric is

$$d\tau^2 = \left(1 + \left(\frac{v_g}{c}\right)^2\right) dt^2 - \frac{1}{c^2} \left[\left(1 + \left(\frac{v_g}{c}\right)^2\right)^{-1} dr^2 + r^2 d\theta^2 + r^2 \sin^2 \theta d\phi^2 \right] \quad (61)$$

and

$$d\tau^2 = \left(1 + \frac{r_g}{r}\right) dt^2 - \frac{1}{c^2} \left[\left(1 + \frac{r_g}{r}\right)^{-1} dr^2 + r^2 d\theta^2 + r^2 \sin^2 \theta d\phi^2 \right] \quad (62)$$

The metrics given by Eqs. (14) and (17) correspond to positive curvature of the intrinsic velocity surface of a particle, and the metrics given by Eqs. (61) and (62) correspond to negative curvature of the intrinsic velocity surface of a particle. In the case of the electrons, the corresponding state is called a hyperbolic electron since the plot of the intrinsic velocity along a unique z-axis is a hyperbolic surface.

M. Hyperbolic Electrons

As shown previously [44], the bound electron acts as a resonator cavity that traps single photons of discrete frequencies. Thus, photon absorption occurs as an excitation of a resonator mode. The photon's electric field superposes that of the proton such that the radial electric field has a magnitude proportional to Z/n at the electron where $n = 1, 2, 3, \dots$ for excited states and

$$n = \frac{1}{2}, \frac{1}{3}, \frac{1}{4}, \dots, \frac{1}{137} \text{ for lower energy states [2, 45] given in the first paper of this series of two$$

[46]. This causes the charge density of the electron to correspondingly decrease and the radius to increase for states higher than 13.6 eV, and the charge density of the electron to correspondingly increase and the radius to decrease for states lower than 13.6 eV.

Photons can propagate electron-surface current and maintain force balance in other excitations as well, such as during Larmor excitation in a magnetic field [47]. Furthermore, photons can exclusively maintain the current of a fundamental particle or a state of a fundamental particle in force balance. An example of the former involves the strong nuclear force wherein heavy photons called gluons can solely maintain the force balance of quarks in baryons [48]. An example of the latter is the observation that free electrons in liquid helium form physical hollow bubbles that serve as resonator cavities that transition to fractional (1/integer) sizes and migrate at different rates when an electric field is applied [10, 49]. Specifically, free electrons are trapped in superfluid helium as autonomous electron bubbles interloped between helium atoms that have been excluded from the space occupied by the bubble. The surrounding helium atoms maintain the spherical bubble through van der Waals forces. The *bubble-like* current-density function called an orbitsphere [43] can act as a resonator cavity. The excitation of the Maxwellian resonator cavity modes by resonant photons form bubbles with radii of reciprocal integer multiples of that of the unexcited $n=1$ state. The central force that results in a fractional electron radius compared to the unexcited electron is provided by the absorbed photon. Each stable excited state electron bubble which has a radius of $\frac{r_1}{\text{integer}}$

may migrate in an applied electric field. The photo-conductivity absorption spectrum of free electrons in superfluid helium and their mobilities predicted from the corresponding size and multipolarity of these long-lived bubble-like states with quantum numbers n , ℓ , and m_ℓ matched the experimental results of the 15 identified ions. Further examples of the existence of free electrons as bubble-like cavities in fluids devoid of any molecules are free electrons in liquid ammonia and in oils [49].

Thus, it is a general phenomenon that photon absorption occurs as an excitation of a resonator mode; consequently, the hydrogen atomic energy states are quantized as a function of the parameter n as shown previously [50]. Each value of n corresponds to an allowed transition caused by a resonant photon which excites the transition of the orbitsphere resonator cavity. Similarly, scattering of electrons with special resonant kinetic energies such as 42.3 eV can result in the excitation of a hyperbolic-electron state—an electron state having a unique trapped photon that maintains the electron in a stable bounded two-dimensional spherical shape with \hbar of angular momentum and a velocity function on the surface whose magnitude approaches the limit of light-speed at opposite poles (Eq. (35.75) of Ref. [51]) corresponding to a negatively-curved two-dimensional velocity surface. The velocity function of the two-dimensional spherical hyperbolic electron is shown in color scale in Figure 1. The velocity distribution along the unique z-axis of a hyperbolic electron is shown schematically in Figure 2.

Energy balance is achieved when the magnitude of the photon field is equivalent to $+e$ at the origin such that the photon-electron electric energy and magnetic energies are balanced by the corresponding self energies [51]. Then, the total energy is the kinetic energy which is equivalent to the initial translational kinetic energy as required for energy conservation. In this case, the de Broglie-relationship is maintained in the formation of a hyperbolic electron from a free electron in the same manner as in the case of the ionization of a bound atomic electron to form a free electron. The radius of the hyperbolic electron is given by balance of the forces corresponding to the energies that satisfy the energy balance and continuity conditions. The outward centrifugal force is balanced by the electric force and the magnetic force [51]. Then, the force balance for the state having quantum numbers $\ell = 0$ $m_\ell = 0$ is

$$\frac{\hbar^2}{m_e r^3} = \frac{e^2}{4\pi\epsilon_0 r^2} + \frac{\hbar^2}{2m_e r^3} \sqrt{s(s+1)} \quad (63)$$

$$r_0 = a_0 \left(1 - \frac{\sqrt{\frac{3}{4}}}{2} \right) = 0.567 a_0 \quad (64)$$

The radii and energies of fifteen hyperbolic electronic states given in Table 2 are calculated using the force balance equation corresponding to Eq. (63) with the additional magnetic forces given by Eqs. (65-67) and linear combinations of these states which conserve the relationship between Coulombic energy and kinetic energy corresponding to Eq. (63) [51]. The magnetic quantum numbers and additional magnetic forces are

For $\ell = 1$ $m_\ell = 0$

$$\mathbf{F}_{orbital} = \frac{1}{3} \frac{\hbar^2}{4m_e r_0^3} \sqrt{s(s+1)} \mathbf{i}_r \quad (65)$$

For $\ell = 1$ $m_\ell = 1$

$$\mathbf{F}_{orbital} = \frac{2}{3} \frac{\hbar^2}{4m_e r_0^3} \sqrt{s(s+1)} \mathbf{i}_r \quad (66)$$

For \mathbf{S}_p corresponding to $\frac{\hbar}{2}$ along the Z-axis

$$\mathbf{F}_{orbital} = \frac{1}{2} \frac{\hbar^2}{4m_e r_0^3} \sqrt{s(s+1)} \mathbf{i}_r \quad (67)$$

Hyperbolic electrons can be formed by crossing an electron beam with a beam of neutral atoms such as helium. The velocity is given by

$$v_z = \frac{\hbar}{m_e \rho_0} = \frac{\hbar}{m_e r_0} \quad (68)$$

where ρ_0 is the radius of the free electron and r_0 is the radius of the corresponding hyperbolic electron calculated from the force balance equation. The kinetic energy of the incident electron that scatters to form a hyperbolic electron is given by

$$T = \frac{1}{2} m_e v_z^2 \quad (69)$$

Hyperbolic electrons can also be formed by inelastic scattering wherein the difference between the incidence energy E_i and the excitation energy E_{loss} of the species with which the free electron collides is one of the resonant production energies T , one of the incident kinetic energies, given in Table 2.

$$T = E_i - E_{loss} \quad (70)$$

The velocities (Eq. (68)) and energies (Eq. (69)) corresponding to the fifteen states are listed in Table 2 with their corresponding radii and quantum numbers.

In the case of a velocity function having negative curvature, the relationship between the energy, mass-energy, and the time differentials given by the combination of Eqs. (20) and (25) becomes

$$\left(1 + \frac{2GM}{rc^2}\right) \frac{dt}{d\tau} = \frac{E}{mc^2} \quad (71)$$

where M is the mass of the Earth and m is the mass of the hyperbolic electron. Consider the case wherein E_o , is the orbital energy of the electron with initial velocity v_0 and kinetic energy E_i :

$$E_i = \frac{1}{2}mv_0^2 \quad (72)$$

where m is the mass of the hyperbolic electron. The orbit is hyperbolic wherein the scattering angle, ϕ , is [51]

$$\phi = 2 \arctan \frac{E_o}{2E_i} \quad (73)$$

The orbital energy E_o of the hyperbolic electron following its production is determined using Eq. (71). Consider Eq. (31) for the conditions of hyperbolic electron production:

$$d\tau = dt \left(1 - \frac{2Gm_0}{c^2 r_\alpha^*} - \frac{v^2}{c^2}\right)^{\frac{1}{2}} \quad (74)$$

Substitution of Eq. (74) into Eq. (71) gives

$$mc^2 \frac{\left(1 + \frac{2GM}{r_\alpha^* c^2}\right)}{\left(1 + \frac{2Gm_0}{c^2 r_\alpha^*} - \frac{v^2}{c^2}\right)^{\frac{1}{2}}} = E \quad (75)$$

where r_α^* is the production radius. The gravitational velocity of the Earth for hyperbolic electron production in the laboratory frame, v_{g_E} , is

$$v_{g_E} = \sqrt{\frac{2GM}{r_\alpha^*}} \quad (76)$$

Then, Eq. (75) becomes

$$mc^2 \frac{\left(1 + \left(\frac{v_{g_E}}{c}\right)^2\right)}{\left(1 + \left(\frac{v_{g_E}}{c}\right)^2 - \frac{v^2}{c^2}\right)^{\frac{1}{2}}} = E \quad (77)$$

The proper and coordinate times are synchronous when

$$v_{g_E} = v \quad (78)$$

Substitution of Eq. (78) into Eq. (77) gives

$$mc^2 \left(1 + \frac{v^2}{c^2}\right) = E \quad (79)$$

Using Eq. (79) and the low-speed kinetic energy equation, the orbital energy is

$$\begin{aligned}
E_o &\approx \left(m_0 c^2 + \frac{1}{2} m_0 v^2 \right) \left(1 + \left(\frac{v}{c} \right)^2 \right) - m_0 c^2 \\
&\approx \frac{1}{2} m_0 v^2 + m c^2 \left(\frac{v}{c} \right)^2 \\
&\approx \frac{3}{2} m_0 v^2
\end{aligned} \tag{80}$$

With the substitution of E_i and E_o given by Eqs. (72) and (79) into Eq. (73), the scattering angle, ϕ , is

$$\begin{aligned}
\phi &= 2 \arctan \frac{\frac{3}{2} m_0 v^2}{2 \frac{1}{2} m_0 v^2} \\
&= 2 \arctan \frac{3}{2} \\
&= 112.6^\circ
\end{aligned} \tag{81}$$

According to Eqs. (32-34) and (38), matter, energy, and spacetime are conserved with respect to creation of the hyperbolic electron which is repelled from a gravitating body (e.g. the Earth). The ejection of a hyperbolic electron having a negatively curved velocity surface from the Earth with an energy given by Eq. (80) at the scattering angle given by Eq. (81) and having a transition radius and time given by Eqs. (83) and (84), must result in an infinitesimal decrease in the radius of the Earth (e.g. r of the Schwarzschild-type metric given by Eq. (20) where $m_0 = M$ is the mass of the Earth, 5.98×10^{24} kg). The amount that the gravitational potential energy of the Earth is lowered is equivalent to the total energy gained by the repelled hyperbolic electron. Momentum is also conserved for the electron, Earth, and scattering atom or molecule wherein the gravitating body that repels the hyperbolic electron, the Earth, receives an equal and opposite change of momentum with respect to that of the electron.

As given previously [20], at particle production, the production photon and created gravitational field front are at light velocity, the particle velocity must be the Newtonian gravitational escape velocity, its energy is zero, and its trajectory is a parabola. In contrast, hyperbolic electron production results in a negatively-curved velocity surface wherein the mass at the extremes approaches light speed. Thus, the hyperbolic-electron-production radius in the light-like frame r_α^{**} is given by the particle-production condition given previously [18], the maximum speed of light at hyperbolic-electron-production for the photon that provides the force balance (Eqs. (63) and (65-67)) and the corresponding outgoing gravitational field front. In this case, the Earth's gravitational velocity is also equal to the speed of light in the production frame. The gravitational velocity of the Earth for hyperbolic electron production in the production frame, v_{gE}^* , is

$$v_{gE}^* = \sqrt{\frac{2GM}{r_\alpha^{**}}} = c \tag{82}$$

Then, the hyperbolic-electron-production radius is

$$r_{\alpha}^{**} = \frac{2GM}{c^2} = r_g = 8.88 \times 10^{-3} \text{ m} \quad (83)$$

where r_g is the gravitational radius. The corresponding production time t_g is

$$t_g = \frac{2\pi r_{\alpha}^{**}}{c} = \frac{4\pi GM}{c^3} = \frac{2\pi r_g}{c} = \frac{2\pi (8.88 \times 10^{-3} \text{ m})}{c} = 1.86 \times 10^{-10} \text{ s} \quad (84)$$

Hyperbolic electrons are formed by scattering at the energies given in Table 2 wherein the scattering is elastic. Hyperbolic electrons can also be formed by inelastic scattering wherein the difference between the incidence energy E_i and the excitation energy E_{loss} of the species with which the free electron collides is one of the resonant production energies T (Eq. (70)), the one of the kinetic energies given in Table 2. Thus, free-electrons made incident on and elastically scattered from target species such as noble-gas atoms (e.g. *He*, *Ne*, *Ar*, *Kr*, and *Xe*) or molecules (e.g. H_2 and N_2) are anticipated to form hyperbolic electrons that accelerate away from the center of the Earth at a threshold energy of 42.3 eV and the additional resonance energies given in Table 2. And, the fifth-force effect will occur at higher incident electron energy as hyperbolic electrons form according to the resonance condition of Eq. (70) due to incident-electron energy loss. The loss may be due to excitation or recoil energy transfer to the collision target, such as a noble gas atom, until a resonant energy given in Table 2 for the scattered free-electrons can no longer be achieved. In the case of a resonant elastic excitation, distinct peaks in the upward-deflected-beam current of an electron are predicted at the incident energies given in Table 2. These predictions have been confirmed experimentally.

II. Experimental

The experimental set up for scattering an electron beam from a crossed atomic beam and measuring the fifth-force deflected beam as the normalized current at a top electrode relative to a bottom electrode is shown in Figure 3. The side, top, and inside views of the fifth-force testing apparatus are shown in Figures 4, 5, and 6, respectively. The beams and electrodes were housed in a stainless steel chamber with two cylindrical μ -metal shields to eliminate the influence of the Earth's magnetic field. The inner μ -metal cylinder had a diameter of 50 mm, and the outer μ -metal cylinder had a diameter of 130 mm. The electron gun was a Kimball Physics ELG-2 (5-2 keV, 1 nA - 10 μ A). In the energy region of 20–160 eV, the typical electron beam spot size was about 0.5 mm at a working distance of 20 mm, the half-width and accuracy of the beam energy were both about ± 1 eV, and the incident beam current was in the range of 100 nA - 1 μ A. A noble-gas atomic beam or molecular beam was produced by flowing the gas (*He*, *Ne*, *Ar*, *Xe*, H_2 , or N_2) into the chamber through a gas nozzle made of quarter inch OD stainless steel tubing and having a 10 micron-diameter orifice positioned 30 mm from the tip of the electron gun. The chamber vacuum pressure before introducing the gas was 5×10^{-7} Torr. The chamber pressure with the introduction of the atomic beam was typically in the range of 1.5×10^{-5} to 6×10^{-5} Torr. The pressure was adjusted to optimize the fifth-force effect. A Faraday cup collected the undeflected portion of the beam. With low charging at the electrodes, the peak current deflected away from the Faraday cup was up to 60% of the incident current observed as peaks at specific energies.

The 20 x 15 mm molybdenum plate electrodes were positioned above and below the beam path perpendicular to the gravitation-force line of the Earth with a separation of 40 mm and

positioned 100 mm and then 50 mm from the gas nozzle to test the fifth force in the far field and near field, respectively. A small Faraday cup to measure the axis beam intensity was positioned 130 mm from the molybdenum plates in the direction of electron beam axis. The scattering angles were about $10\text{-}13^\circ$ and $18\text{-}27^\circ$ for the 100 mm and 50 mm position, respectively. The upper and bottom plates were each connected to a pico-ammeter for current measurement. The upper and bottom plates were each connected to a pico-ammeter for current measurement. Before introducing the gas into the chamber, the axial electron beam intensity was optimized for each energy position as the energy was stepped over the range of 10 eV to 160 eV at 1 eV intervals with a dwell time of 5 seconds per position. The electron beam energy, electron gun focusing, and beam deflection voltages were controlled by the power supply system and PC software. The scattering current intensities at both electrodes were recorded as a function of the electron beam energy.

III. Results and Discussion of Tests on the Fifth Force

A. Far-Field Results

The current at the upper electrode normalized by that at the bottom electrode when the electron beam was incident with a helium, neon, argon, krypton, and xenon atomic beam and a hydrogen and nitrogen molecular beam compared to the absence of the atomic beam at a flight distance of 100 mm is shown in Figures 7-13, respectively. No energy-dependent bias in the beam current was present as indicated by the flat ratio of upper and bottom electrode currents in the absence of the atomic or molecular beam. The ratio was close to unity over the measured energy range for all experiments involving the controls of all gases indicating that the beam was well centered. In contrast, when the atomic or molecular beam was introduced, a striking upward deflection of the beam was observed as an increased current at the upper and a decreased at current at the lower electrode giving a normalized ratio significantly greater than that in the absence of the atomic beam. Furthermore, a series of peaks were observed that matched the theoretical predictions for the formation of some of the hyperbolic-electronic states given in Table 2. The peak assignments for helium, neon, argon, krypton, xenon, hydrogen and nitrogen are given in Tables 3-9, respectively. Peaks with an expected high transition probability such as that corresponding to the $n=1\ S_p$ state at 64.7 eV were strong; whereas, peaks involving low probability such as the 48.3 eV peak corresponding to the $(\ell=0\ m_\ell=0) + (\ell=1\ m_\ell=0)$ state involving a double excitation were low. The fifth-force effect continued at higher incident electron energy with decreasing intensity in agreement with the decreased cross section for energy loss to match the condition of Eq. (70).

Typically, the peak intensities were a maximum at a pressure of about 3.5×10^{-5} Torr and a beam current of about 100 nA. Furthermore, it was observed that the intensity of the hyperbolic-electronic-state peaks decreased in intensity after the first scan and the lower-intensity spectrum was extremely reproducible thereafter. This observation was found to be due to the differential deflection that gives a charging differential. Once charging occurred, greater intensity peaks were observed as the pressure was increased over a range of about a factor of two since the gas partially discharged the electrodes. The charging effect could also be partially compensated for with an increase in beam current over a range of 30% since it increased the upward current due to the higher probability for electron scattering as the number of electrons increases. Since the ratio of the beam currents in the absence of the atomic or molecular beam

was observed to be about one over the energy range and energy peaks are observed, the charging does not eliminate the fifth-force effect, but only dampens it. It was also found that inelastic interference was not a significant issue in observing the predicted resonant peaks corresponding to the fifth-force effect, even in the case of scattering from a molecular beam in the far field. Molecules have many continua bands in their absorption spectra. But, inelastic scattering of the incident electron beam using a molecular beam was not appreciable as shown by the observation of intense resonant peaks shown in Figures 12 and 13.

B. Near-field results

The distance of the electrodes from the beam intersection point was decreased from 100 mm to 50 mm. It was found that considerably more charging of the upper electrode occurred in the 50 mm case as expected which required a higher gas pressure of about 5×10^{-5} to obtain good spectra. Charging was evidenced by the dramatic decrease in the spectral intensity upon repeat scanning with significant broadening of the peaks. Only after a significant delay between scans was the intensity recovered. This effect is shown for neon in comparing Figures 15 and 16. This is an indication that the half-life of a hyperbolic state can be very long (> 1 min). In addition, it was found that certain lines of the spectra changed their relative intensity with pressure. And, the lower-energy as compared to higher-energy peaks dominated the spectrum depending on the whether the electron gun was maintained at high energy (200 V) or low energy (10 V), respectively, as the chamber was extensively pumped. This would be expected if collisional depopulation of these states having large half-lives was dependent on the energy of the state and that of the collisional partner or secondary electrons or ions to which energy is transferred. An example of this effect is shown for *Xe* in Figure 19.

The gun energy was set to 10 V with extensive pumping with gas flow at pressure between scans to enhance the high-energy region of the spectrum. But, even at this condition, there appeared to be a bias for the higher-energy range of the spectrum in the 50 mm case. Based on the vector projections of the velocity of Eqs. (80-81), the upward acceleration due to the fifth force increases with the kinetic energy of production of the hyperbolic electrons. Thus, it is expected that the higher-energy states dominate the spectrum in the near field and the lower-energy states dominate in the far field. To test this prediction, the 50 mm results were compared to the corresponding 100 mm results. Specifically, the upper-electrode current normalized by that at the bottom electrode when the electron beam was incident with a helium, neon, argon, krypton, and xenon atomic beam and a hydrogen and nitrogen molecular beam compared to the absence of the atomic beam is shown in Figures 7-13 with peak assignments given in Tables 3-9, respectively. The predicted trend is apparent when these results are compared to the corresponding 50 mm results given in Figures 14-21 and Tables 10-17.

With optimization of the pressure condition, a very large fifth-force effect was observed as measured by the percentage of the incident current involved. With *Xe*, the current at the Faraday cup dropped to less than half the incident current at 55 eV, 74 eV and 81 eV as the pressure was increased to an optimized value. These peaks did not match ionization energies of xenon or sum thereof. The sharp dips in Faraday current corresponded to the peaks for the $\ell=1 m_\ell=0$, $\ell=1 m_\ell=1$, and $(S_p + \ell=1 m_\ell=0) + (\ell=1 m_\ell=0)$ state formation showing very strong resonance production with this scatterer and the sets of conditions run. The effect was repeated with *Kr* which showed a sharp dip in the Faraday current of about half the incident current at 74 eV corresponding to the peak for the $\ell=1 m_\ell=1$ state formation. The same dip

but of less intensity was observed with Ne , and a small dip ($\sim 15\%$) was also observed at $55 eV$, $74 eV$, and $81 eV$ with Ar . The trend was $Xe > Kr > Ar > Ne$ as expected based on the geometric cross sections. This effect occurred as the pressure was increased to an optimum of about 5.5×10^{-5} Torr. As with the other gases, the intensities of the peaks of the electrode current ratios were pressure dependent, but the presence of peaks at predicted energies was 100% reproducible.

C. Acceleration Due to the Fifth Force

The magnitude of the fifth force can be conservatively calculated from the deflection distance and time of flight of the hyperbolic electrons to the upper electrode in the far-field case (100 mm transit distance). The time of flight to the electrodes after the scattering event to form a hyperbolic electron can be estimated from the transit distance Δz by

$$t = \frac{\Delta z}{v_{z0}} \quad (85)$$

Then, the acceleration due to the fifth force is given by

$$a = \frac{2\Delta x}{t^2} = \frac{2\Delta x}{\left(\frac{\Delta z}{v_{z0}}\right)^2} = 2\Delta x \left(\frac{v_{z0}}{\Delta z}\right)^2 \quad (86)$$

where Δx is the vertical distance from the beam axis to the top electrode. The dimensions of the apparatus are shown in Figure 22. With the threshold resonant incident electron kinetic energy of $42.3 eV$, the electron velocity is $v_{z0} = 3.86 \times 10^6 m/s$ (Eqs. (64) and (68-69)). Then, using $\Delta z = 0.1 m$ and $\Delta x = 0.02 m$ in Eqs. (85) and (86), the flight time and fifth-force acceleration are

$$t = \frac{\Delta z}{v_{z0}} = \left(\frac{0.1 m}{3.86 \times 10^6 m/s}\right) = 2.59 \times 10^{-8} s \quad (87)$$

$$a_x = 2\Delta x \left(\frac{v_{z0}}{\Delta z}\right)^2 = 2(0.02 m) \left(\frac{3.86 \times 10^6 m/s}{0.1 m}\right)^2 = 5.96 \times 10^{13} m/s^2 \quad (88)$$

The electron velocity upon reaching the upper plate is

$$v_x = a_x t = (5.96 \times 10^{13} m/s^2)(2.59 \times 10^{-8} s) = 1.54 \times 10^6 m/s \quad (89)$$

and the corresponding energy is

$$T = \frac{1}{2} m_e v_x^2 = \frac{1}{2} m_e (1.54 \times 10^6 m/s)^2 = 6.77 eV \quad (90)$$

As a comparison with the fifth-force acceleration given by Eq. (88), the acceleration due to gravity is only $9.8 m/s^2$. The fifth-force acceleration based on this estimate is over twelve orders of magnitude greater. As one application, even a micro fifth-force device has great promise as a replacement for micro-ion-thrusters for maintaining the orbits of satellites.

References

1. R. L. Mills, *The Grand Unified Theory of Classical Quantum Mechanics*, October 2007 Edition, BlackLight Power, Inc., Cranbury, New Jersey, posted at www.blacklightpower.com.
2. R.L. Mills, "Physical Solutions of the Nature of the Atom, Photon, and Their Interactions to Form Excited and Predicted Hydrino States," *Physics Essays*, in press.

3. R. L. Mills, "The Nature of the Chemical Bond Revisited and an Alternative Maxwellian Approach", *Physics Essays*, Vol. 17, No. 3, (2004), pp. 342-389.
4. R. L. Mills, "Classical Quantum Mechanics", *Physics Essays*, Vol. 16, No. 4, December, (2003), pp. 433-498.
5. R. L. Mills, "Exact Classical Quantum Mechanical Solutions for One- Through Twenty-Electron Atoms", *Physics Essays*, in press.
6. R. L. Mills, "Maxwell's Equations and QED: Which is Fact and Which is Fiction", *Physics Essays*, in press.
7. R. L. Mills, "Exact Classical Quantum Mechanical Solution for Atomic Helium Which Predicts Conjugate Parameters from a Unique Solution for the First Time", submitted.
8. R. L. Mills, "The Fallacy of Feynman's Argument on the Stability of the Hydrogen Atom According to Quantum Mechanics", *Annales de la Fondation Louis de Broglie*, Vol. 30, No. 2, (2005), pp. 129-151.
9. R. Mills, "The Grand Unified Theory of Classical Quantum Mechanics", *Int. J. Hydrogen Energy*, Vol. 27, No. 5, (2002), pp. 565-590.
10. R. L. Mills, "The Nature of Free Electrons in Superfluid Helium--a Test of Quantum Mechanics and a Basis to Review its Foundations and Make a Comparison to Classical Theory", *Int. J. Hydrogen Energy*, Vol. 26, No. 10, (2001), pp. 1059-1096.
11. R. Mills, "The Grand Unified Theory of Classical Quantum Mechanics", Global Foundation, Inc. Orbis Scientiae entitled *The Role of Attractive and Repulsive Gravitational Forces in Cosmic Acceleration of Particles The Origin of the Cosmic Gamma Ray Bursts*, (29th Conference on High Energy Physics and Cosmology Since 1964) Dr. Behram N. Kursunoglu, Chairman, December 14-17, 2000, Lago Mar Resort, Fort Lauderdale, FL, Kluwer Academic/Plenum Publishers, New York, pp. 243-258.
12. E. Giannetto, "The rise of special relativity: Henri Poincaré's works before Einstein. Atti del 18 Congresso di Storia della Fisica e Dell'Astronomia, (1998), pp. 171-207, [<http://www.brera.unimi.it/old/Atti-Como-98/Giannetto.pdf>].
13. E. Giannetto, "The rise of special relativity: Henri Poincaré's works before Einstein. Atti del 18 Congresso di Storia della Fisica e Dell'Astronomia, (1998), p. 179, [<http://www.brera.unimi.it/old/Atti-Como-98/Giannetto.pdf>].
14. H. Poincaré, "L'état actuel et l'avenir de la physique mathématique," *Bulletin des sciences mathématiques*, Vol. 28, (1904), pp.302-324; quoted in Whittaker (1987), p. 30.
15. E. Whittaker, *A History of the Theories of Aether and Electricity*, Vol. 2, Modern Theories, Chapter 2, "The Relativity Theories of Poincaré and Lorentz", Nelson, London, (1987), Reprinted, American Institute of Physics, pp. 30-31.
16. S. Kak, "Moving observers in an isotropic universe", *International Journal of Theoretical Physics*, Vol. 46, (2007).
17. J. D. Jackson, *Classical Electrodynamics*, Second Edition, John Wiley & Sons, New York, (1975), pp. 739-752.
18. Reference 1, Gravity section.
19. Reference 1, Unification of Spacetime, the Forces, Matter, and Energy section.
20. Reference 1, Leptons section and Quarks section.
21. L. Z. Fang, and R. Ruffini, *Basic Concepts in Relativistic Astrophysics*, World Scientific, (1983).
22. G. R. Fowles, *Analytical Mechanics*, Third Edition, Holt, Rinehart, and Winston, New York, (1977), pp. 154-155.

23. Reference 1, Photon section.
24. J. D. Jackson, *Classical Electrodynamics*, Second Edition, John Wiley & Sons, New York, (1975), pp. 739-779.
25. K. Hagiwara et al., Phys. Rev. D 66, 010001 (2002); <http://pdg.lbl.gov/2002/s035.pdf>.
26. P. J. Mohr and B. N. Taylor, "CODATA recommended values of the fundamental physical constants: 1998", *Reviews of Modern Physics*, Vol. 72, No. 2, April, (2000), pp. 351-495.
27. Reference 1, Gravity and Relationship of Matter to Energy and Spacetime Expansion sections.
28. J. C. Mather, E. S. Cheng, A preliminary measurement of the cosmic microwave background spectrum by the Cosmic Background Explorer (COBE) satellite, *Astrophysical Journal Letters*, Vol. 354, L37-L40 (May 10, 1990).
29. W. Saunders, C. Frenk, The density field of the local universe; *Nature*, 349(6304), 32-38 (1991).
30. R. P. Kirshner, A. Oemler, Jr., P. L. Schechter, S. A. Shectman, A deep survey of galaxies, *Astronomical Journal*, 88, 1285-1300 (September 1983).
31. V. de Lapparent, M. J. Geller, J. P. Huchra, The mean density and two-point correlation function for the CfA redshift survey slices, *Astrophysical Journal*, 332(9) 44-56 (1988).
32. A. Dressler, S. M. Faber, D. Burstein, R. L. Davies, D. Lynden-Bell, R. J. Terlevich, G. Wegner, "Spectroscopy and photometry of elliptical galaxies—A large-scale streaming motion in the local universe", *Astrophysical Journal*, 313, L37-L42, (1987).
33. S. Flamsteed, Crisis in the Cosmos, *Discover*, 16(3), 66(1995).
34. J. Glanz, CO in the early universe clouds cosmologists' views, *Science*, 273(5275), 581 (1996).
35. S. D. Landy, Mapping the Universe, *Scientific American*, 280(6), 38-45 (1999).
36. R. L. Mills, *The Grand Unified Theory of Classical Quantum Mechanics*, November 1995 Edition, HydroCatalysis Power Corp., Malvern, PA, Library of Congress Catalog Number 94-077780, ISBN number ISBN 0-9635171-1-2, Chp. 22.
37. E. G. Adelberger, C. W. Stubbs, B. R. Heckel, Y. Su, H. E. Swanson, G. Smith, J. H. Gundlach, Phys. Rev. D, Vol. 42, No. 10, (1990), pp. 3267-3292.
38. Reference 1, Equivalence of Inertial and Gravitational Masses Due to Absolute Space and Absolute Light Velocity section.
39. A. Beiser, *Concepts of Modern Physics*, Fourth Edition, McGraw-Hill Book Company, New York, (1978), pp. 2-40.
40. R. M. Wald, *General Relativity*, University of Chicago Press, Chicago, (1984), pp. 91-101.
41. N. A. Bahcall, J. P. Ostriker, S. Perlmutter, P. J. Steinhardt, *Science*, May 28, 1999, Vol. 284, pp. 1481-1488.
42. F. C. Witteborn, W. M. and Fairbank, *Physical Review Letters*, Vol. 19, No. 18, (1967), pp. 1049-1052.
43. Reference 1, One-Electron Atom section.
44. Reference 1, Excited States of the One-Electron Atom (Quantization) section.
45. R. Mills, J. He, Z. Chang, W. Good, Y. Lu, B. Dhandapani, "Catalysis of Atomic Hydrogen to Novel Hydrogen Species $H^-(1/4)$ and $H_2(1/4)$ as a New Power Source", *Int. J. Hydrogen Energy*, Vol. 32, No. 12, (2007), pp. 2573-2584.
46. R. L. Mills, G. Zhao, K. Akhar, R. Chang, J. He, Y. Lu, M. Nansteel, W. Good, B. Dhandapani, "Commercializable Power Source from Forming New States of Hydrogen", to be submitted.

47. Reference 1, Magnetic Parameters of the Electron (Bohr Magneton) section.
48. Reference 1, Quark and Gluon Functions section.
49. Reference 1, Stability of Fractional-Principal-Quantum States of Free Electrons in Liquid Helium section.
50. Reference 1, Excited States (Quantization) section.
51. Reference 1, Fifth Force section.

Table 1. The calculated relations between the lepton masses and neutron to electron mass ratio are given in terms of the dimensionless fine structure constant α only and compared to experimental values from the 1998 CODATA and the Particle Data Group given in parentheses [12-13].

$$\frac{m_\mu}{m_e} = \left(\frac{\alpha^{-2}}{2\pi}\right)^{\frac{2}{3}} \frac{\left(1 + 2\pi \frac{\alpha^2}{2}\right)}{\left(1 + \frac{\alpha}{2}\right)} = 206.76828 \quad (206.76827)$$

$$\frac{m_\tau}{m_\mu} = \left(\frac{\alpha^{-1}}{2}\right)^{\frac{2}{3}} \frac{\left(1 + \frac{\alpha}{2}\right)}{\left(1 - 4\pi\alpha^2\right)} = 16.817 \quad (16.817)$$

$$\frac{m_\tau}{m_e} = \left(\frac{\alpha^{-3}}{4\pi}\right)^{\frac{2}{3}} \frac{\left(1 + 2\pi \frac{\alpha^2}{2}\right)}{\left(1 - 4\pi\alpha^2\right)} = 3477.2 \quad (3477.3)$$

$$\frac{m_N}{m_e} = \frac{12\pi^2}{1-\alpha} \sqrt{\frac{\sqrt{3}}{\alpha}} \frac{\left(1 + 2\pi \frac{\alpha^2}{2}\right)}{\left(1 - 2\pi \frac{\alpha^2}{2}\right)} = 1838.67 \quad (1838.68)$$

Table 2. The theoretical velocities and the kinetic energies of incident elastically scattered electrons for resonant hyperbolic electron formation given in increasing order of energy with the corresponding radii and quantum numbers of the $n = 1$ hyperbolic-electronic states.

Peak #	Theoretical Hyperbolic-Electron Radius (a_0)	Theoretical Velocity (10^6 m/s)	Theoretical Threshold Kinetic Energy (eV)	Quantum Numbers \mathbf{S}_p , ℓ , and m_ℓ
1	0.5670	3.8584	42.32	$\ell = 0 \quad m_\ell = 0$
2	0.5309	4.1207	48.27	$(\ell = 0 \quad m_\ell = 0) + (\ell = 1 \quad m_\ell = 0)$
3	0.4948	4.4212	55.57	$\ell = 1 \quad m_\ell = 0$
4	0.4768	4.5885	59.85	$S_p + (\ell = 1 \quad m_\ell = 0)$
5	0.4587	4.7690	64.65	\mathbf{S}_p
6	0.4407	4.9642	70.06	$S_p + (\ell = 1 \quad m_\ell = 1)$
7	0.4226	5.1761	76.17	$\ell = 1 \quad m_\ell = 1$
8	0.4136	5.2890	79.52	$((\mathbf{S}_p + \ell = 1 \quad m_\ell = 0) + (\ell = 1 \quad m_\ell = 0))$ $+ (\ell = 1 \quad m_\ell = 1)$
9	0.4046	5.4069	83.11	$(\mathbf{S}_p + \ell = 1 \quad m_\ell = 0) + (\ell = 1 \quad m_\ell = 0)$
10	0.3866	5.6593	91.05	$((\mathbf{S}_p + \ell = 1 \quad m_\ell = 0) + (\ell = 1 \quad m_\ell = 0))$ $+ ((\mathbf{S}_p + \ell = 1 \quad m_\ell = 1) + (\ell = 1 \quad m_\ell = 0))$
11	0.3685	5.9364	100.18	$(\mathbf{S}_p + \ell = 1 \quad m_\ell = 1) + (\ell = 1 \quad m_\ell = 0)$
12	0.3505	6.2420	110.76	$((\mathbf{S}_p + \ell = 1 \quad m_\ell = 1) + (\ell = 1 \quad m_\ell = 0))$ $+ ((\mathbf{S}_p + \ell = 1 \quad m_\ell = 0) + (\ell = 1 \quad m_\ell = 1))$
13	0.3324	6.5807	123.11	$(\mathbf{S}_p + \ell = 1 \quad m_\ell = 0) + (\ell = 1 \quad m_\ell = 1)$
14	0.3144	6.9584	137.65	$((\mathbf{S}_p + \ell = 1 \quad m_\ell = 0) + (\ell = 1 \quad m_\ell = 1))$ $+ ((\mathbf{S}_p + \ell = 1 \quad m_\ell = 1) + (\ell = 1 \quad m_\ell = 1))$
15	0.2964	7.3820	154.92	$(\mathbf{S}_p + \ell = 1 \quad m_\ell = 1) + (\ell = 1 \quad m_\ell = 1)$

Table 3. The assignment of the incident electron energy peaks observed in the normalized upwardly deflected electron beam elastically scattered from a helium atomic beam to theoretical energies and the corresponding quantum numbers of $n = 1$ resonant hyperbolic-electronic states.

Peak #	Observed Peak Energy (eV)	Theoretical Threshold Kinetic Energy (eV)	Quantum Numbers \mathbf{S}_p , ℓ , and m_ℓ
1	47	42.32	$\ell = 0$ $m_\ell = 0$
3	55	55.57	$\ell = 1$ $m_\ell = 0$
5	65	64.65	\mathbf{S}_p

Table 4. The assignment of the incident electron energy peaks observed in the normalized upwardly deflected electron beam elastically scattered from a neon atomic beam to theoretical energies and the corresponding quantum numbers of $n = 1$ resonant hyperbolic-electronic states.

Peak #	Observed Peak Energy (eV)	Theoretical Threshold Kinetic Energy (eV)	Quantum Numbers \mathbf{S}_p , ℓ , and m_ℓ
1	45	42.32	$\ell = 0$ $m_\ell = 0$
3	55	55.57	$\ell = 1$ $m_\ell = 0$
5	66	64.65	\mathbf{S}_p
6	72	70.06	$S_p + (\ell = 1 \ m_\ell = 1)$
7	78	76.17	$\ell = 1 \ m_\ell = 1$

Table 5. The assignment of the incident electron energy peaks observed in the normalized upwardly deflected electron beam elastically scattered from an argon atomic beam to theoretical energies and the corresponding quantum numbers of $n = 1$ resonant hyperbolic-electronic states.

Peak #	Observed Peak Energy (eV)	Theoretical Threshold Kinetic Energy (eV)	Quantum Numbers \mathbf{S}_p , ℓ , and m_ℓ
1	45	42.32	$\ell = 0 \quad m_\ell = 0$
2	49	48.27	$(\ell = 0 \quad m_\ell = 0) + (\ell = 1 \quad m_\ell = 0)$
3	55	55.57	$\ell = 1 \quad m_\ell = 0$
4	59	59.85	$S_p + (\ell = 1 \quad m_\ell = 0)$
5	67	64.65	\mathbf{S}_p
6	72	70.06	$S_p + (\ell = 1 \quad m_\ell = 1)$
7	78	76.17	$\ell = 1 \quad m_\ell = 1$

Table 6. The assignment of the incident electron energy peaks observed in the normalized upwardly deflected electron beam elastically scattered from a krypton atomic beam to theoretical energies and the corresponding quantum numbers of $n = 1$ resonant hyperbolic-electronic states.

Peak #	Observed Peak Energy (eV)	Theoretical Threshold Kinetic Energy (eV)	Quantum Numbers \mathbf{S}_p , ℓ , and m_ℓ
1	45	42.32	$\ell = 0$ $m_\ell = 0$
3	55	55.57	$\ell = 1$ $m_\ell = 0$
4	60	59.85	$S_p + (\ell = 1 \ m_\ell = 0)$
5	67	64.65	\mathbf{S}_p
6	72	70.06	$S_p + (\ell = 1 \ m_\ell = 1)$

Table 7. The assignment of the incident electron energy peaks observed in the normalized upwardly deflected electron beam elastically scattered from a xenon atomic beam to theoretical energies and the corresponding quantum numbers of $n = 1$ resonant hyperbolic-electronic states.

Peak #	Observed Peak Energy (eV)	Theoretical Threshold Kinetic Energy (eV)	Quantum Numbers \mathbf{S}_p , ℓ , and m_ℓ
1	46	42.32	$\ell = 0 \quad m_\ell = 0$
4	60	59.85	$S_p + (\ell = 1 \quad m_\ell = 0)$
5	67	64.65	\mathbf{S}_p
6	72	70.06	$S_p + (\ell = 1 \quad m_\ell = 1)$
7	78	76.17	$\ell = 1 \quad m_\ell = 1$

Table 8. The assignment of the incident electron energy peaks observed in the normalized upwardly deflected electron beam elastically scattered from a hydrogen molecular beam to theoretical energies and the corresponding quantum numbers of $n=1$ resonant hyperbolic-electronic states.

Peak #	Observed Peak Energy (eV)	Theoretical Threshold Kinetic Energy (eV)	Quantum Numbers \mathbf{S}_p , ℓ , and m_ℓ
1	45	42.32	$\ell = 0$ $m_\ell = 0$
3	55	55.57	$\ell = 1$ $m_\ell = 0$
5	67	64.65	\mathbf{S}_p
6	72	70.06	$S_p + (\ell = 1 \ m_\ell = 1)$
7	78	76.17	$\ell = 1 \ m_\ell = 1$

Table 9. The assignment of the incident electron energy peaks observed in the normalized upwardly deflected electron beam elastically scattered from a nitrogen molecular beam to theoretical energies and the corresponding quantum numbers of $n=1$ resonant hyperbolic-electronic states.

Peak #	Observed Peak Energy (eV)	Theoretical Threshold Kinetic Energy (eV)	Quantum Numbers \mathbf{S}_p , ℓ , and m_ℓ
1	45	42.32	$\ell = 0$ $m_\ell = 0$
3	55	55.57	$\ell = 1$ $m_\ell = 0$
5	67	64.65	\mathbf{S}_p
6	72	70.06	$S_p + (\ell = 1 \ m_\ell = 1)$
7	78	76.17	$\ell = 1 \ m_\ell = 1$

Table 10. The assignment of the incident electron energy peaks observed in the normalized upwardly deflected electron beam elastically scattered from a helium atomic beam to theoretical energies and the corresponding quantum numbers of $n = 1$ resonant hyperbolic-electronic states.

Peak #	Observed Peak Energy (eV)	Theoretical Threshold Kinetic Energy (eV)	Quantum Numbers \mathbf{S}_p , ℓ , and m_ℓ
5	65	64.65	\mathbf{S}_p
7	76	76.17	$\ell = 1 \ m_\ell = 1$
9	82	83.11	$(\mathbf{S}_p + \ell = 1 \ m_\ell = 0) + (\ell = 1 \ m_\ell = 0)$
11	100	100.18	$(\mathbf{S}_p + \ell = 1 \ m_\ell = 1) + (\ell = 1 \ m_\ell = 0)$

Table 11. The assignment of the incident electron energy peaks observed in the normalized upwardly deflected electron beam elastically scattered from a neon atomic beam to theoretical energies and the corresponding quantum numbers of $n = 1$ resonant hyperbolic-electronic states.

Peak #	Observed Peak Energy (eV)	Theoretical Threshold Kinetic Energy (eV)	Quantum Numbers \mathbf{S}_p , ℓ , and m_ℓ
9	83	83.11	$(\mathbf{S}_p + \ell = 1 \ m_\ell = 0) + (\ell = 1 \ m_\ell = 0)$
11	99	100.18	$(\mathbf{S}_p + \ell = 1 \ m_\ell = 1) + (\ell = 1 \ m_\ell = 0)$
12	109	110.76	$((\mathbf{S}_p + \ell = 1 \ m_\ell = 1) + (\ell = 1 \ m_\ell = 0))$ $+ ((\mathbf{S}_p + \ell = 1 \ m_\ell = 0) + (\ell = 1 \ m_\ell = 1))$
13	120	123.11	$(\mathbf{S}_p + \ell = 1 \ m_\ell = 0) + (\ell = 1 \ m_\ell = 1)$
14	136	137.65	$((\mathbf{S}_p + \ell = 1 \ m_\ell = 0) + (\ell = 1 \ m_\ell = 1))$ $+ ((\mathbf{S}_p + \ell = 1 \ m_\ell = 1) + (\ell = 1 \ m_\ell = 1))$
15	150	154.92	$(\mathbf{S}_p + \ell = 1 \ m_\ell = 1) + (\ell = 1 \ m_\ell = 1)$

Table 12. The assignment of the incident electron energy peaks observed in the normalized upwardly deflected electron beam elastically scattered from a neon atomic beam to theoretical energies and the corresponding quantum numbers of $n = 1$ resonant hyperbolic-electronic states.

Peak #	Observed Peak Energy (eV)	Theoretical Threshold Kinetic Energy (eV)	Quantum Numbers \mathbf{S}_p , ℓ , and m_ℓ
11	100	100.18	$(\mathbf{S}_p + \ell = 1 \ m_\ell = 1) + (\ell = 1 \ m_\ell = 0)$

Table 13. The assignment of the incident electron energy peaks observed in the normalized upwardly deflected electron beam elastically scattered from an argon atomic beam to theoretical energies and the corresponding quantum numbers of $n = 1$ resonant hyperbolic-electronic states.

Peak #	Observed Peak Energy (eV)	Theoretical Threshold Kinetic Energy (eV)	Quantum Numbers \mathbf{S}_p , ℓ , and m_ℓ
3	55	55.57	$\ell = 1 \quad m_\ell = 0$
4	61	59.85	$\mathbf{S}_p + (\ell = 1 \quad m_\ell = 0)$
7	77	76.17	$\ell = 1 \quad m_\ell = 1$

Table 14. The assignment of the incident electron energy peaks observed in the normalized upwardly deflected electron beam elastically scattered from a krypton atomic beam to theoretical energies and the corresponding quantum numbers of $n = 1$ resonant hyperbolic-electronic states.

Peak #	Observed Peak Energy (eV)	Theoretical Threshold Kinetic Energy (eV)	Quantum Numbers \mathbf{S}_p , ℓ , and m_ℓ
6	69	70.06	$\mathbf{S}_p + (\ell = 1 \ m_\ell = 1)$
7	78	76.17	$\ell = 1 \ m_\ell = 1$
9	82	83.11	$(\mathbf{S}_p + \ell = 1 \ m_\ell = 0) + (\ell = 1 \ m_\ell = 0)$

Table 15. The assignment of the incident electron energy peaks observed in the normalized upwardly deflected electron beam elastically scattered from a xenon atomic beam to theoretical energies and the corresponding quantum numbers of $n = 1$ resonant hyperbolic-electronic states.

Peak #	Observed Peak Energy (eV)	Theoretical Threshold Kinetic Energy (eV)	Quantum Numbers \mathbf{S}_p , ℓ , and m_ℓ
1	45	42.32	$\ell = 0 \quad m_\ell = 0$
2	48	48.27	$(\ell = 0 \quad m_\ell = 0) + (\ell = 1 \quad m_\ell = 0)$
6	69	70.06	$S_p + (\ell = 1 \quad m_\ell = 1)$
8	79	79.52	$((\mathbf{S}_p + \ell = 1 \quad m_\ell = 0) + (\ell = 1 \quad m_\ell = 0))$ $+ (\ell = 1 \quad m_\ell = 1)$
9	82	83.11	$(\mathbf{S}_p + \ell = 1 \quad m_\ell = 0) + (\ell = 1 \quad m_\ell = 0)$
10	91	91.05	$((\mathbf{S}_p + \ell = 1 \quad m_\ell = 0) + (\ell = 1 \quad m_\ell = 0))$ $+ ((\mathbf{S}_p + \ell = 1 \quad m_\ell = 1) + (\ell = 1 \quad m_\ell = 0))$

Table 16. The assignment of the incident electron energy peaks observed in the normalized upwardly deflected electron beam elastically scattered from a hydrogen molecular beam to theoretical energies and the corresponding quantum numbers of $n=1$ resonant hyperbolic-electronic states.

Peak #	Observed Peak Energy (eV)	Theoretical Threshold Kinetic Energy (eV)	Quantum Numbers \mathbf{S}_p , ℓ , and m_ℓ
3	55	55.57	$\ell = 1 \quad m_\ell = 0$
4	61	59.85	$S_p + (\ell = 1 \quad m_\ell = 0)$
9	83	83.11	$(\mathbf{S}_p + \ell = 1 \quad m_\ell = 0) + (\ell = 1 \quad m_\ell = 0)$
11	99	100.18	$(\mathbf{S}_p + \ell = 1 \quad m_\ell = 1) + (\ell = 1 \quad m_\ell = 0)$
12	109	110.76	$((\mathbf{S}_p + \ell = 1 \quad m_\ell = 1) + (\ell = 1 \quad m_\ell = 0))$ $+ ((\mathbf{S}_p + \ell = 1 \quad m_\ell = 0) + (\ell = 1 \quad m_\ell = 1))$
13	120	123.11	$(\mathbf{S}_p + \ell = 1 \quad m_\ell = 0) + (\ell = 1 \quad m_\ell = 1)$
14	135	137.65	$((\mathbf{S}_p + \ell = 1 \quad m_\ell = 0) + (\ell = 1 \quad m_\ell = 1))$ $+ ((\mathbf{S}_p + \ell = 1 \quad m_\ell = 1) + (\ell = 1 \quad m_\ell = 1))$

Table 17. The assignment of the incident electron energy peaks observed in the normalized upwardly deflected electron beam elastically scattered from a nitrogen molecular beam to theoretical energies and the corresponding quantum numbers of $n=1$ resonant hyperbolic-electronic states.

Peak #	Observed Peak Energy (eV)	Theoretical Threshold Kinetic Energy (eV)	Quantum Numbers \mathbf{S}_p , ℓ , and m_ℓ
3	55	55.57	$\ell = 1 \ m_\ell = 0$
4	61	59.85	$S_p + (\ell = 1 \ m_\ell = 0)$
9	83	83.11	$(\mathbf{S}_p + \ell = 1 \ m_\ell = 0) + (\ell = 1 \ m_\ell = 0)$
11	99	100.18	$(\mathbf{S}_p + \ell = 1 \ m_\ell = 1) + (\ell = 1 \ m_\ell = 0)$
12	109	110.76	$((\mathbf{S}_p + \ell = 1 \ m_\ell = 1) + (\ell = 1 \ m_\ell = 0))$ $+ ((\mathbf{S}_p + \ell = 1 \ m_\ell = 0) + (\ell = 1 \ m_\ell = 1))$
13	120	123.11	$(\mathbf{S}_p + \ell = 1 \ m_\ell = 0) + (\ell = 1 \ m_\ell = 1)$

Figure 1. The hyperbolic electron is a two-dimensional spherical shell of mass (charge)-density having a velocity function that is maximum at the $\pm z$ -axis with $\theta = 0$ and $\theta = \pi$ and minimum at the in the xy -plane at $\theta = \pi/2$.

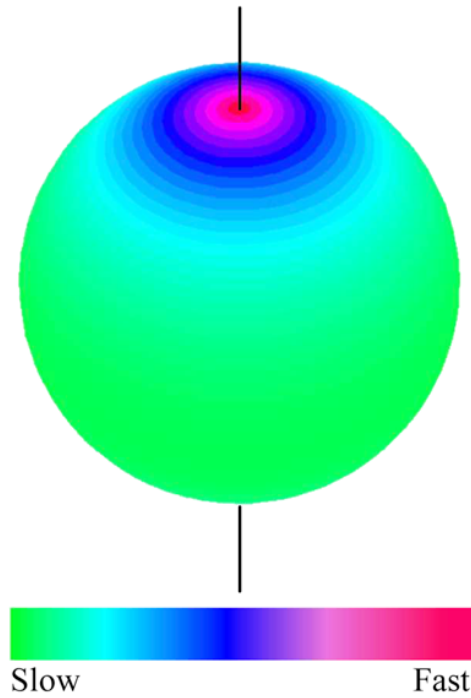


Figure 2. The magnitude of the velocity distribution ($|\mathbf{v}_\phi|$) on a two-dimensional sphere along the z -axis (vertical axis) of a hyperbolic electron.

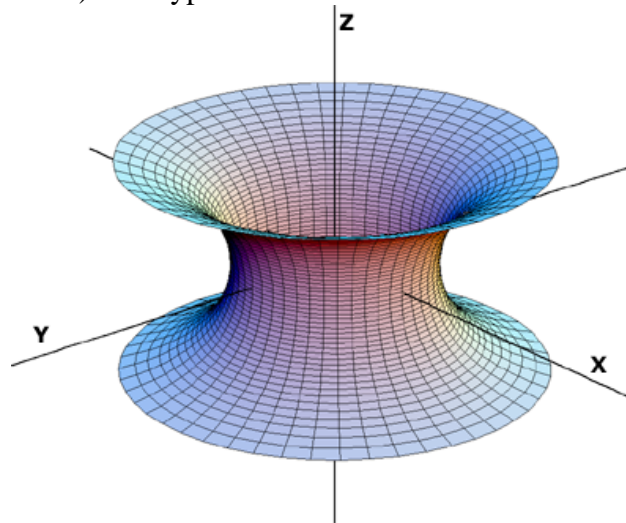


Figure 3. Schematic of the apparatus for scattering an electron beam from a crossed atomic or molecular beam and measuring the fifth-force deflected beam as the normalized current at a top electrode relative to a bottom electrode.

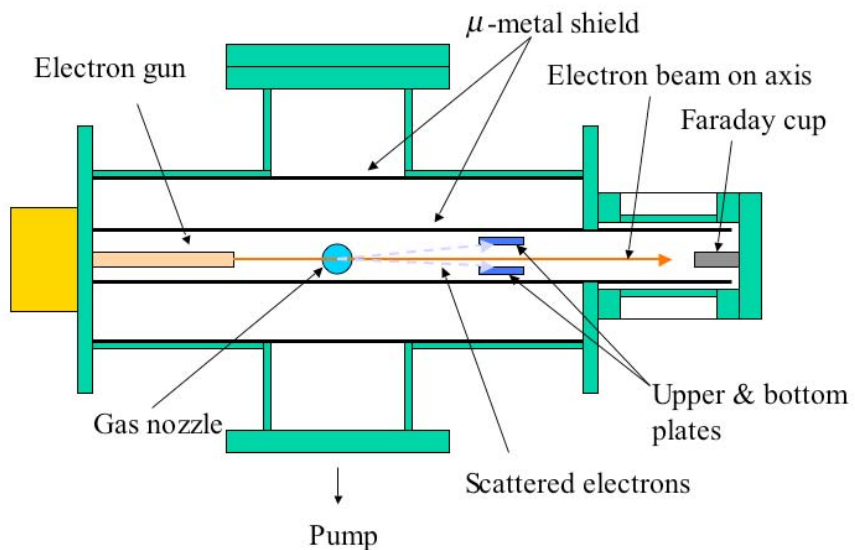


Figure 4. Side view of the apparatus for scattering an electron beam from a crossed atomic or molecular beam and measuring the fifth-force deflected beam.

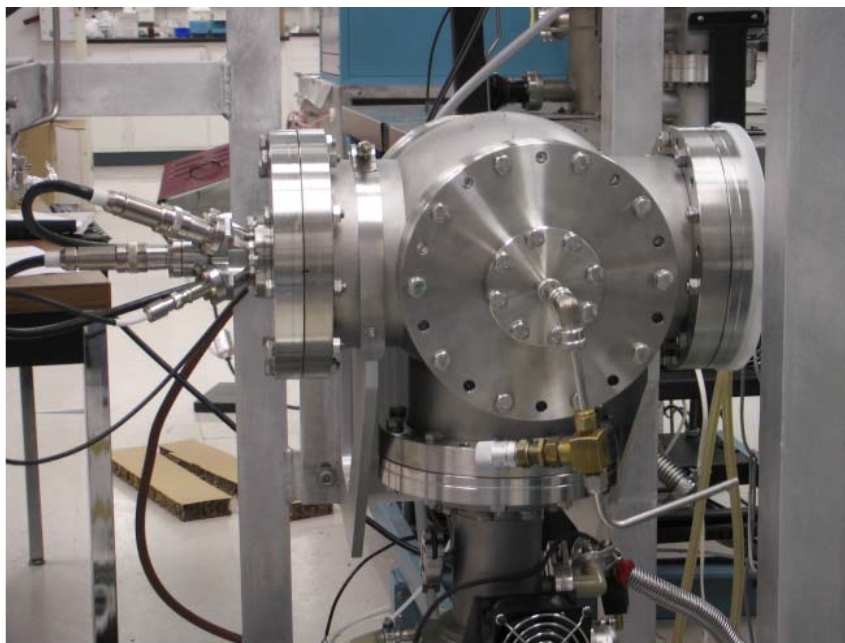


Figure 5. Top view of the apparatus for scattering an electron beam from a crossed atomic or molecular beam and measuring the fifth-force deflected beam.

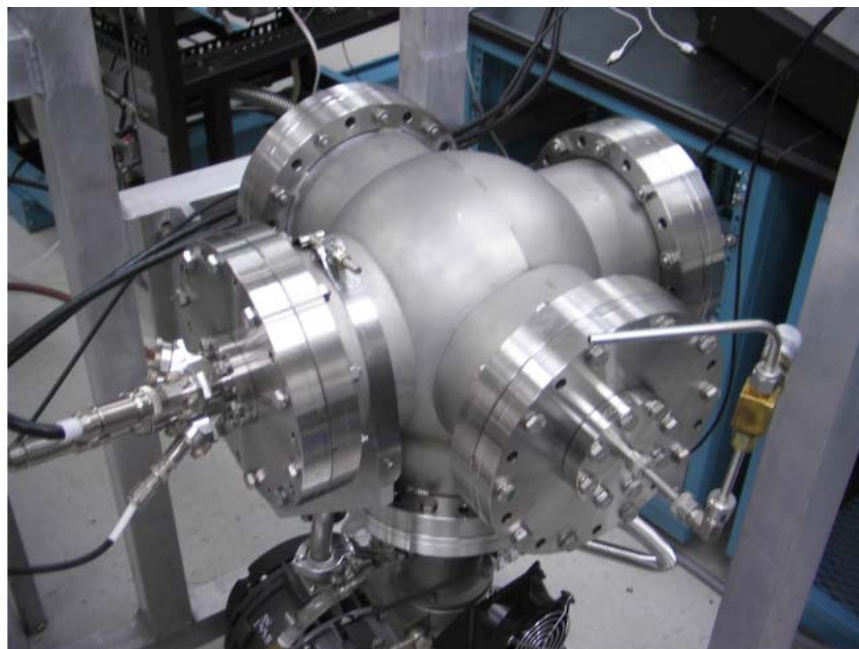


Figure 6. Inside view of the apparatus for scattering an electron beam from a crossed atomic or molecular beam and measuring the fifth-force deflected beam showing the electron gun, gas nozzle, and top and bottom electrodes.

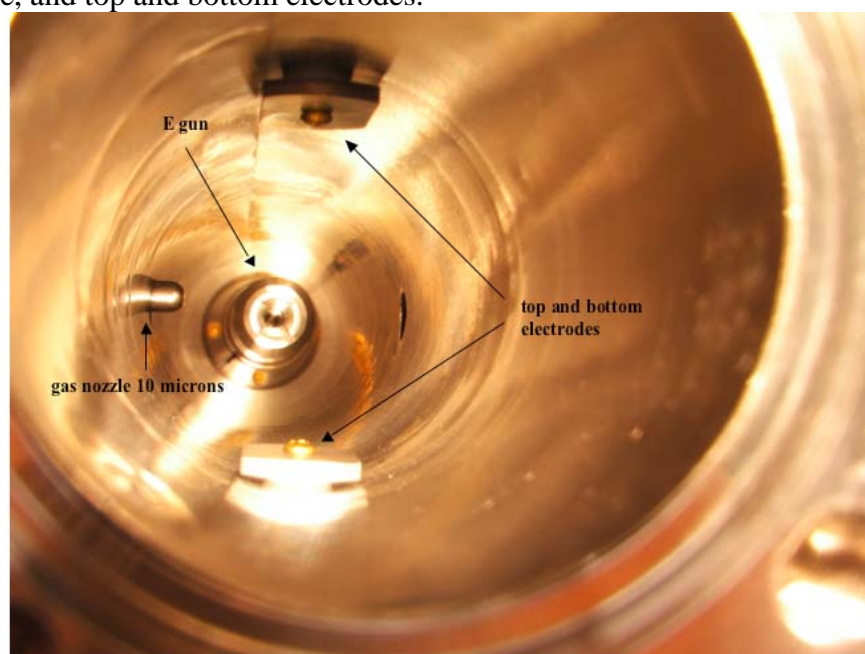


Figure 7. The current at the top electrode divided by that at the bottom for the scattering an electron beam from a crossed helium beam (blue curve) compared to the same ratio in the absence of the helium atomic beam (red curve) at a flight distance of 100 mm. A significant fifth-force effect was observed.

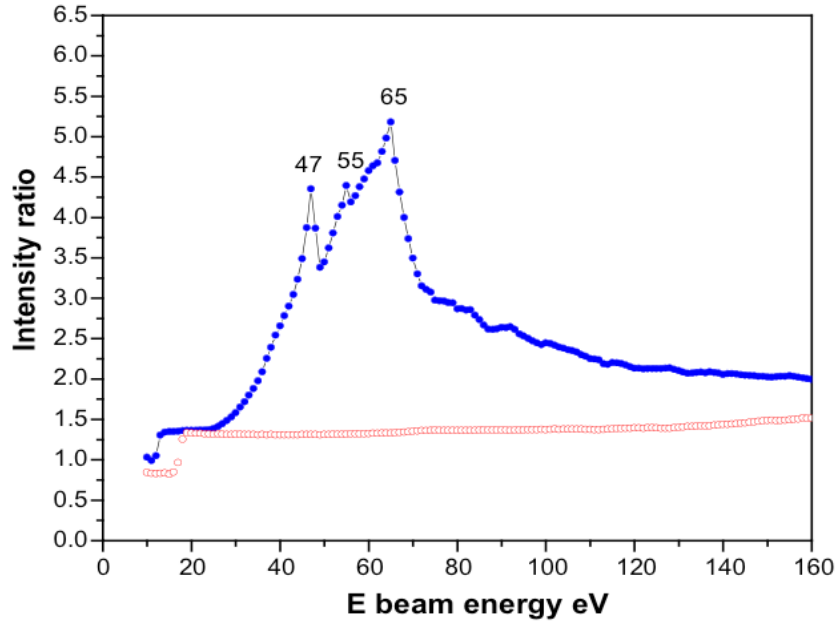


Figure 8. The current at the top electrode divided by that at the bottom for the scattering an electron beam from a crossed neon beam (blue curve) compared to the same ratio in the absence of the neon atomic beam (red curve) at a flight distance of 100 mm. A significant fifth-force effect was observed. The S_p hyperbolic-electronic state at 66 eV dominated the spectrum indicating that the neon atom's electronic transitions do not interfere significantly with the resonant production of hyperbolic electrons of this state at the corresponding energy.

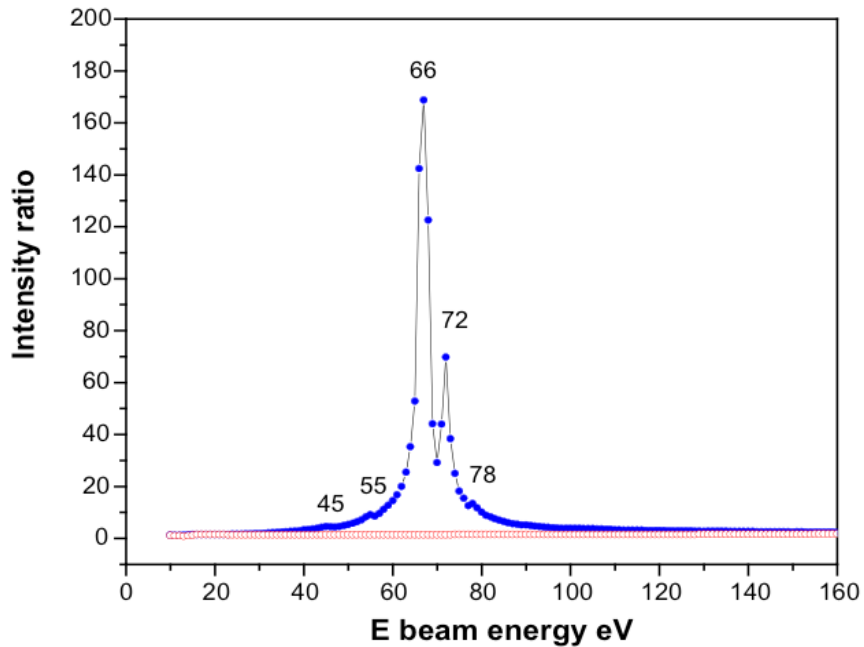


Figure 9. The current at the top electrode divided by that at the bottom for the scattering an electron beam from a crossed argon beam (blue curve) compared to the same ratio in the absence of the argon atomic beam (red curve) at a flight distance of 100 mm. A significant fifth-force effect was observed. All of the lower-energy hyperbolic-electronic-state transitions of Table 2 were observed at their anticipated relative intensities indicating that the argon atom's electronic transitions do not interfere significantly with the resonant production of hyperbolic electrons.

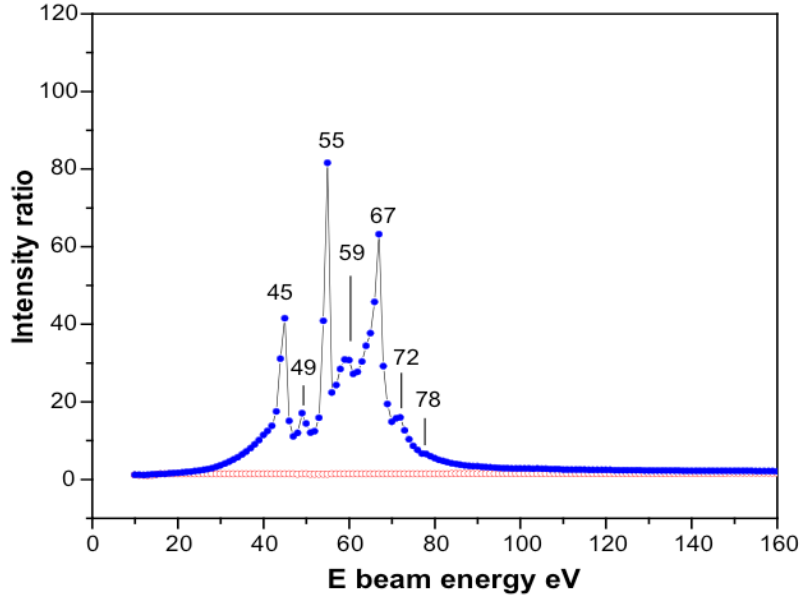


Figure 10. The current at the top electrode divided by that at the bottom for the scattering an electron beam from a crossed krypton atomic beam (blue curve) compared to the same ratio in the absence of the atomic beam (red curve) at a flight distance of 100 mm. A significant fifth-force effect was observed as a dominant peak corresponding to the minimum energy hyperbolic-electronic state.

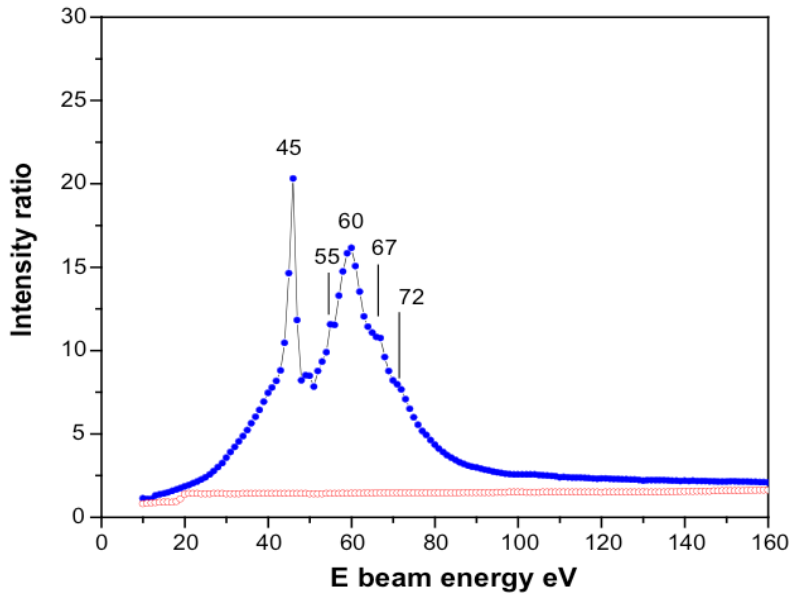


Figure 11. The current at the top electrode divided by that at the bottom for the scattering an electron beam from a crossed xenon beam (blue curve) compared to the same ratio in the absence of the xenon atomic beam (red curve) at a flight distance of 100 mm. As in the case with krypton, a significant fifth-force effect was observed as a dominant peak corresponding to the minimum energy hyperbolic-electronic state.

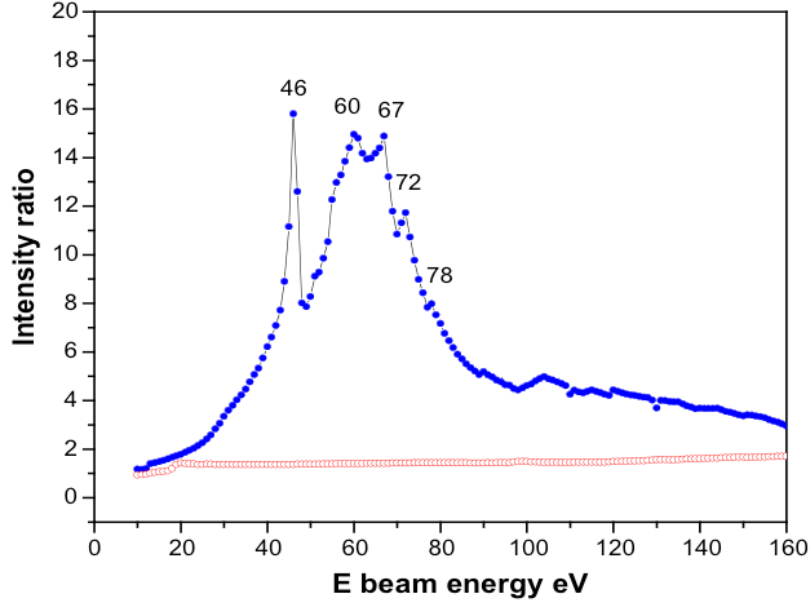


Figure 12. The current at the top electrode divided by that at the bottom for the scattering an electron beam from a crossed hydrogen molecular beam (blue curve) compared to the same ratio in the absence of the H_2 molecular beam (red curve) at a flight distance of 100 mm. The S_p hyperbolic-electronic state at 67 eV dominated the spectrum similar to the case of neon.

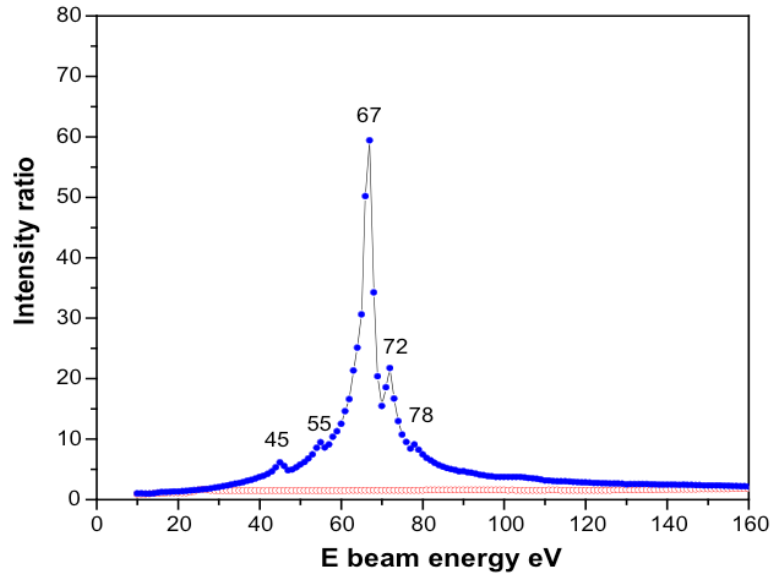


Figure 13. The current at the top electrode divided by that at the bottom for the scattering an electron beam from a crossed nitrogen molecular beam (blue curve) compared to the same ratio in the absence of the N_2 molecular beam (red curve) at a flight distance of 100 mm. As in the case of neon and H_2 , a significant fifth-force effect was observed with the S_p hyperbolic-electronic state at 67 eV dominating the spectrum.

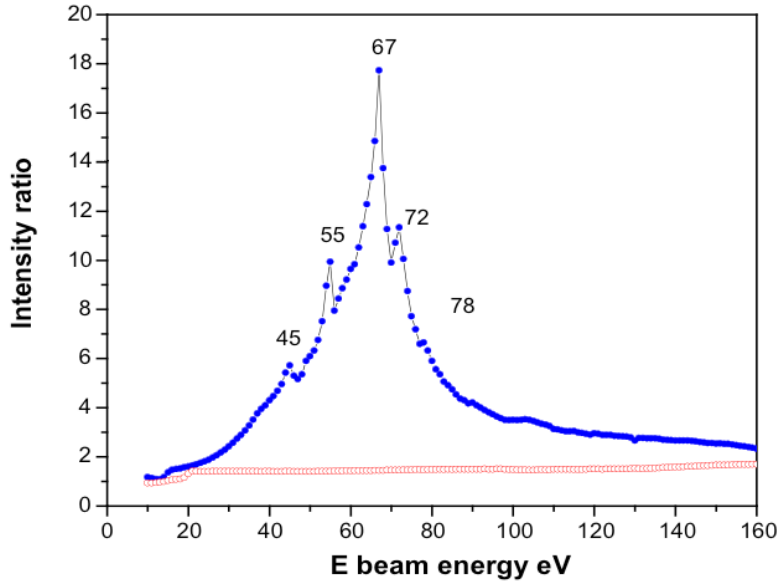


Figure 14. The current at the top electrode divided by that at the bottom for the scattering an electron beam from a crossed helium beam (blue curve) compared to the same ratio in the absence of the helium atomic beam (red curve) at a flight distance of 50 mm. A significant fifth-force effect was observed. The high-energy $(S_p + \ell = 1 m_\ell = 1) + (\ell = 1 m_\ell = 0)$ state was observed at 100 eV, and intense peaks corresponding to the $\ell = 1 m_\ell = 1$, and $(S_p + \ell = 1 m_\ell = 0) + (\ell = 1 m_\ell = 0)$ hyperbolic-electronic states were observed at 76 eV and 82 eV, respectively, indicating that the higher energy states dominate the spectrum in the near field.

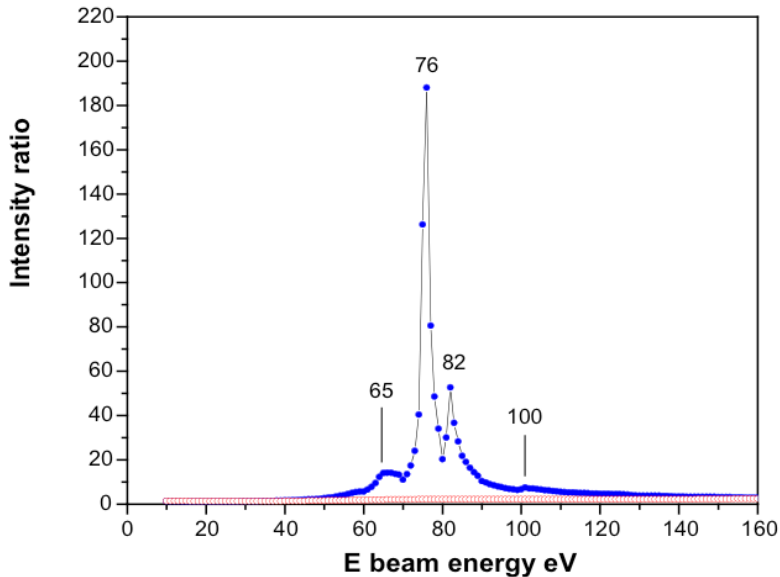


Figure 15. The current at the top electrode divided by that at the bottom for the scattering an electron beam from a crossed neon beam (blue curve) compared to the same ratio in the absence of the neon atomic beam (red curve) at a flight distance of 50 mm. A significant fifth-force effect was observed. The spectrum was very similar to that of H_2 and N_2 showing the series of the highest-energy states from 83 eV to 150 eV in the near field.

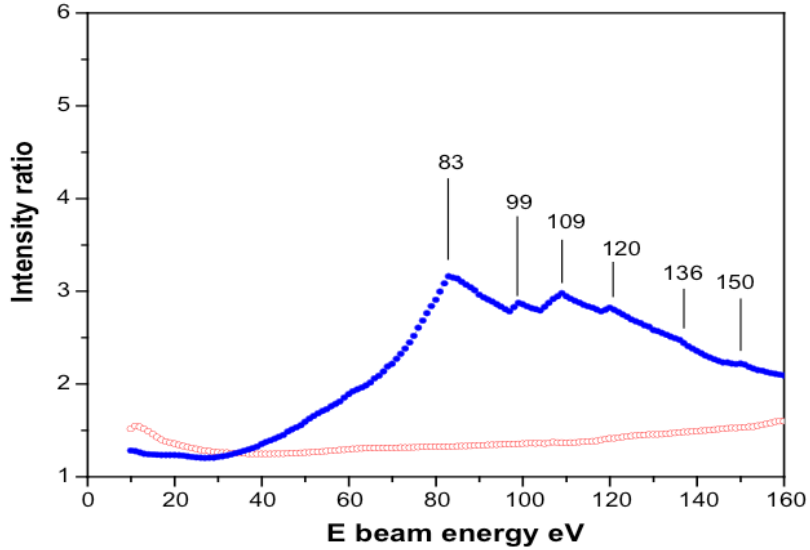


Figure 16. The current at the top electrode divided by that at the bottom for the scattering an electron beam from a crossed neon beam (gray curve) compared to the same ratio in the absence of the neon atomic beam (red curve) at a flight distance of 50 mm. The chamber was cleared by extensive pumping with flow to obtain a scan showing a strong resonance at 100 eV corresponding to the $(S_p + \ell = 1 m_\ell = 1) + (\ell = 1 m_\ell = 0)$ hyperbolic-electronic state that dominated other peaks in the spectrum.

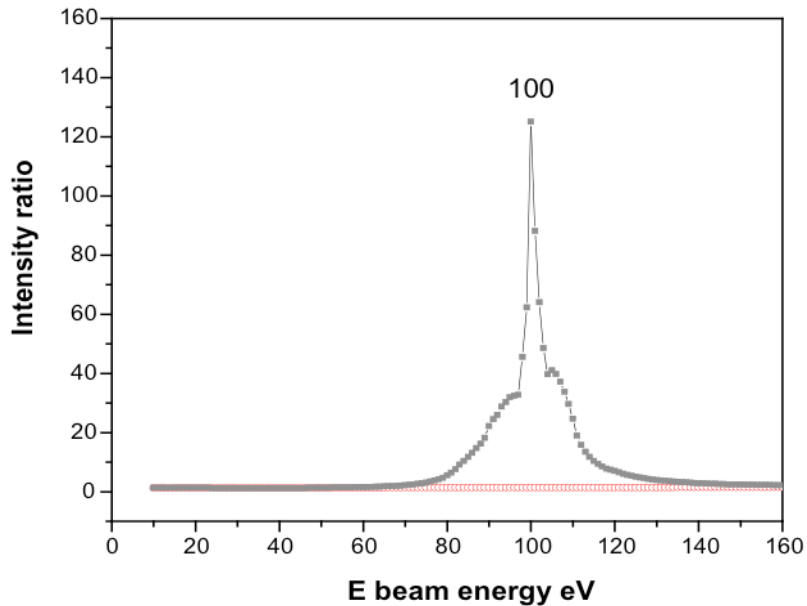


Figure 17. The current at the top electrode divided by that at the bottom for the scattering an electron beam from a crossed argon beam (blue curve) compared to the same ratio in the absence of the argon atomic beam (red curve) at a flight distance of 50 mm. A significant fifth-force effect was observed. The high-energy $\ell = 1$ $m_\ell = 1$ hyperbolic-electronic state at 77 eV was significantly increased in the near field relative to the far field.

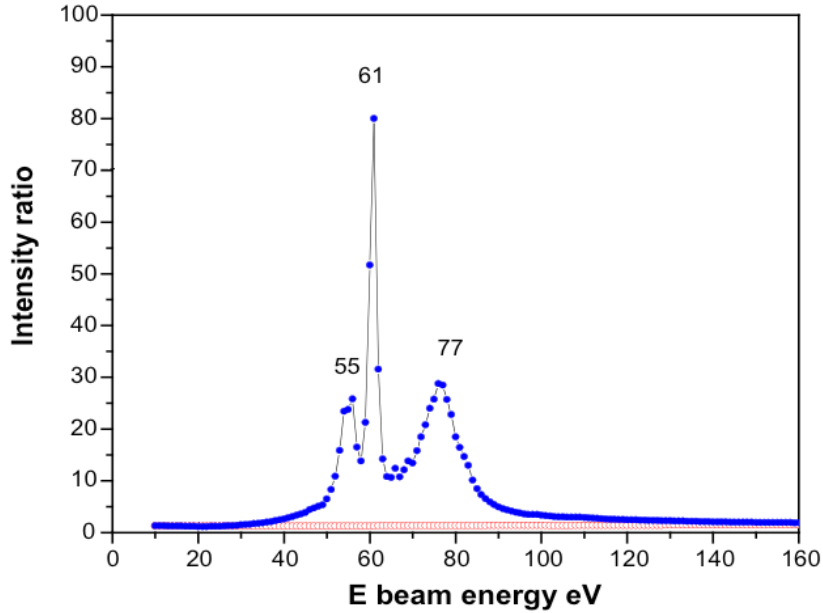


Figure 18. The current at the top electrode divided by that at the bottom for the scattering an electron beam from a crossed krypton atomic beam (blue curve) compared to the same ratio in the absence of the atomic beam (red curve) at a flight distance of 50 mm. A significant fifth-force effect was observed with the spectrum shifted to high-energy hyperbolic-electronic states relative to the far field pattern.

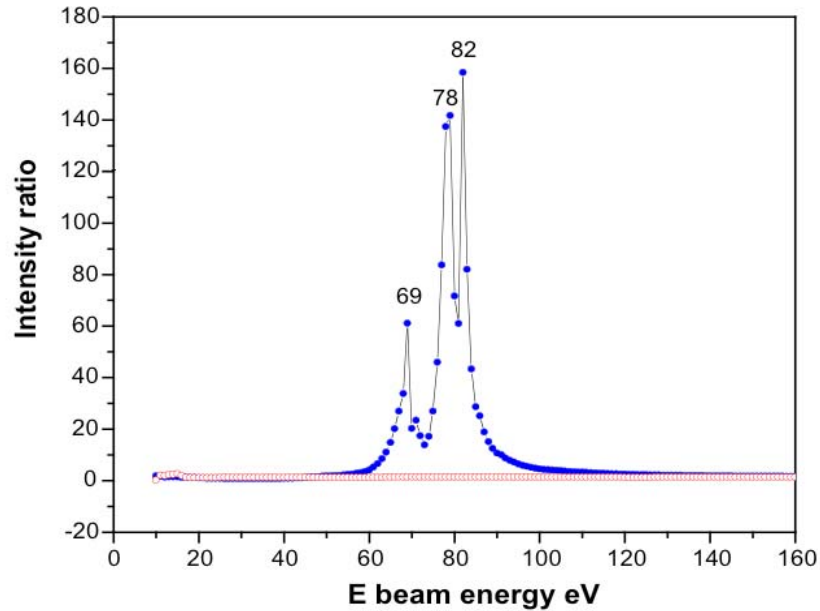


Figure 19. The current at the top electrode divided by that at the bottom for the scattering an electron beam from a crossed xenon beam (top curves) compared to the same ratio in the absence of the xenon atomic beam (bottom curve) at a flight distance of 50 mm. With extensive pumping, the gas-flow was maintained constant at the intermediate pressure of 4.4×10^{-5} Torr while the electron gun was run at 10 V and 200 V before the scans corresponding to the squares and circles, respectively. There was a reciprocal relationship between the gun energy during pumping and the energy range of the spectrum when subsequently acquired.

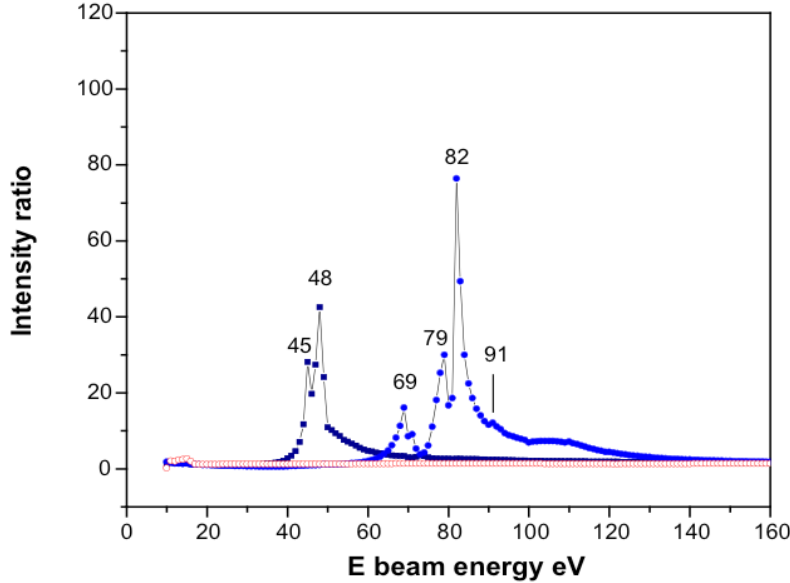


Figure 20. The current at the top electrode divided by that at the bottom for the scattering an electron beam from a crossed hydrogen molecular beam (blue curve) compared to the same ratio in the absence of the H_2 molecular beam (red curve) at a flight distance of 50 mm. A significant fifth-force effect was observed. The spectrum was similar to that of neon with the series of high-energy states out to the $((S_p + \ell = 1 \ m_\ell = 0) + (\ell = 1 \ m_\ell = 1)) + ((S_p + \ell = 1 \ m_\ell = 1) + (\ell = 1 \ m_\ell = 1))$ state observed at 135 eV indicating that the higher energy states dominate the spectrum in the near field.

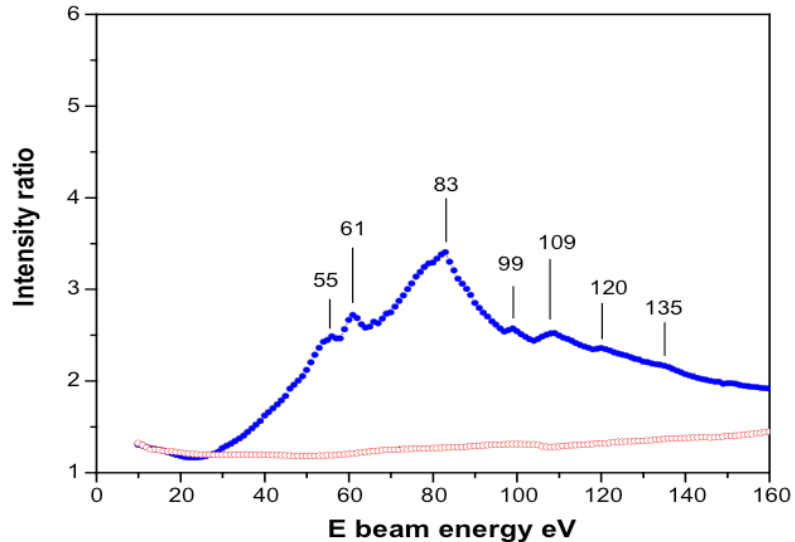


Figure 21. The current at the top electrode divided by that at the bottom for the scattering an electron beam from a crossed nitrogen molecular beam (blue curve) compared to the same ratio in the absence of the N_2 molecular beam (red curve) at a flight distance of 50 mm. The spectrum was essentially the same as that of H_2 with the high-energy states out to the $(S_p + \ell = 1 \ m_\ell = 0) + (\ell = 1 \ m_\ell = 1)$ state observed at 120 eV indicating that the higher energy states dominate the spectrum in the near field.

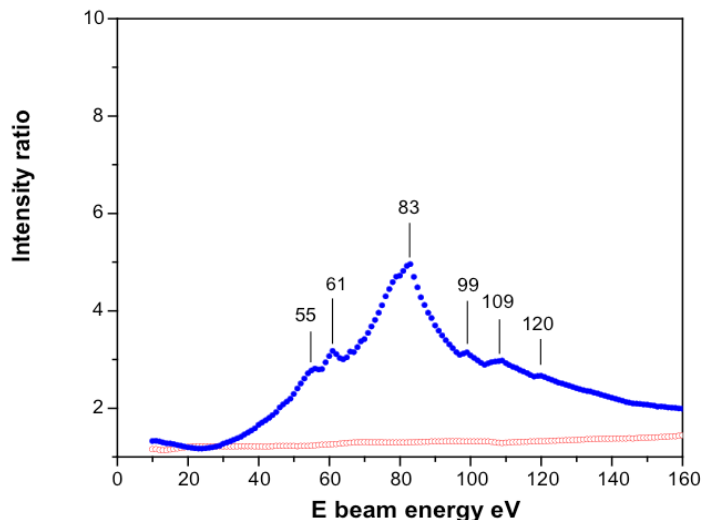


Figure 22. Schematic of the apparatus for scattering an electron beam from a crossed atomic or molecular beam and measuring the fifth-force deflected beam showing the separation of between the intersection point of the beams and top and bottom electrodes at a flight distance of 100 mm. When the flight distance is reduced to 50 mm, the deflection angle from the point of scattering to the electrodes doubles to the range $\sim 18\text{-}27^\circ$.

